# NAVAL POSTGRADUATE SCHOOL
## Monterey, California


# THESIS



TEST AND EVALUATION OF
SURF FORECASTING MODEL

by

Nasuh Cacina

September 1989

Thesis Advisor — Edward B. Thornton
Co-Advisor — Chung-Shang Wu

Unclassified

security classification of this page

## REPORT DOCUMENTATION PAGE

| | | | |
|---|---|---|---|
| 1a Report Security Classification: Unclassified | | 1b Restrictive Markings | |
| 2a Security Classification Authority | | 3 Distribution Availability of Report: Approved for public release; distribution is unlimited. | |
| 2b Declassification Downgrading Schedule | | | |
| 4 Performing Organization Report Number(s) | | 5 Monitoring Organization Report Number(s) | |
| 6a Name of Performing Organization: Naval Postgraduate School | 6b Office Symbol (*if applicable*): 35 | 7a Name of Monitoring Organization: Naval Postgraduate School | |
| 6c Address (*city, state, and ZIP code*): Monterey, CA 93943-5000 | | 7b Address (*city, state, and ZIP code*): Monterey, CA 93943-5000 | |
| 8a Name of Funding Sponsoring Organization | 8b Office Symbol (*if applicable*) | 9 Procurement Instrument Identification Number | |
| 8c Address (*city, state, and ZIP code*) | | 10 Source of Funding Numbers | |
| | | Program Element No | Project No / Task No / Work Unit Accession No |

11 Title (*Include security classification*): TEST AND EVALUATION OF SURF FORECASTING MODEL

12 Personal Author(s): Nasuh Cacina

| 13a Type of Report | 13b Time Covered | 14 Date of Report (*year, month, day*) | 15 Page Count |
|---|---|---|---|
| Master's Thesis | From To | September 1989 | 50 |

16 Supplementary Notation: The views expressed in this thesis are those of the author and do not reflect the official policy or position of the Department of Defense or the U.S. Government.

| 17 Cosati Codes | | | 18 Subject Terms (*continue on reverse if necessary and identify by block number*) |
|---|---|---|---|
| Field | Group | Subgroup | surf,bore formulation,wave height,longshore currents |
| | | | |
| | | | |


19 Abstract (*continue on reverse if necessary and identify by block number*)

A model forecasting the wave height and the longshore current distribution inside the surf zone based on the formulations by Thornton and Guza (1983), (1986), are applied to an extensive set of both laboratory and field data for the purposes of testing and modification. The models are tested on planar beaches as well as barred beaches for a variety of wave conditions.

The wave transformation model is based on solving the energy flux equation using a bore dissipation mechanism and describing the random wave heights with the Rayleigh distribution. The two model parameters B and $\gamma$, where B describes the amount of foam of a breaking wave and $\gamma$ is the proportionality constant which relates the rms wave height to the water depth, are combined into a single parameter BG. The combined parameter BG is shown to be a function of deep water surf similarity parameter. Applied to the present data sets, the rms error of the measured wave height and the model predicted wave height was usually less than 9% and ranged from 1.5% to 15.7% with a mean of 5.3% and a standard deviation of 3.1% for the whole 74 data sets. The wave transformation model is highly robust in describing the wave height distribution in the surf zone.

The longshore current model is based on solving the steady state, alongshore momentum balance for straight and parallel contours using the radiation stress concept. The model requires specifying the bed shear stress coefficient ($c_f$) and turbulent mixing coefficient (N). Applied to the present data sets the rms error between the measured and modeled longshore current values ranged from 4.5% to 55.5% with a mean of 24.6%. The turbulent mixing is not required for planar beaches, but it is required for barred beaches to describe the longshore currents inside the surf zone. The mean value of the bed shear stress coefficient for the present longshore current data is 0.006 and the mean lateral mixing coefficient is 0.006.


| 20 Distribution Availability of Abstract | 21 Abstract Security Classification | |
|---|---|---|
| ☒ unclassified unlimited ☐ same as report ☐ DTIC users | Unclassified | |
| 22a Name of Responsible Individual: Edward B. Thornton | 22b Telephone (*include Area code*): (408) 646-2847 | 22c Office Symbol: 68TM |

DD FORM 1473,84 MAR 83 APR edition may be used until exhausted
All other editions are obsolete

security classification of this page

Unclassified

Approved for public release; distribution is unlimited.

Test And Evaluation Of
Surf Forecasting Model

by

Nasuh Cacina
Lieutenant, Turkish Navy
B.S., Naval Academy, Istanbul, 1983

Submitted in partial fulfillment of the
requirements for the degree of

MASTER OF SCIENCE IN PHYSICAL OCEANOGRAPHY

from the

NAVAL POSTGRADUATE SCHOOL
September 1989

Au

Nasuh Cacina

Approved by:

Edward B. Thornton

Edward B. Thornton, Thesis Advisor

Chung-Shang Wu

Chung-Shang Wu, Co-Advisor

Edward B. Thornton

Curtis A. Collins, Chairman,
Department of Oceanography

## ABSTRACT

A model forecasting the wave height and the longshore current distribution inside the surf zone based on the formulations by Thornton and Guza (1983), (1986), are applied to an extensive set of both laboratory and field data for the purposes of testing and modification. The models are tested on planar beaches as well as barred beaches for a variety of wave conditions.

The wave transformation model is based on solving the energy flux equation using a bore dissipation mechanism and describing the random wave heights with the Rayleigh distribution. The two model parameters, B and $\gamma$, where B describes the amount of foam of a breaking wave and $\gamma$ is the proportionality constant which relates the rms wave height to the water depth, are combined into a single parameter BG. The combined parameter BG is shown to be a function of deep water surf similarity parameter. Applied to the present data sets, the rms error of the measured wave height and the model predicted wave height was usually less than 9% and ranged from 1.5% to 15.7% with a mean of 5.3% and a standard deviation of 3.1% for the whole 74 data sets. The wave transformation model is highly robust in describing the wave height distribution in the surf zone.

The longshore current model is based on solving the steady state, alongshore momentum balance for straight and parallel contours using the radiation stress concept. The model requires specifying the bed shear stress coefficient ($c_f$) and turbulent mixing coefficients ($\varepsilon_y$). Applied to the present data sets the rms error between the measured and modeled longshore current values ranged from 4.5% to 55.5% with a mean of 24.6%. The turbulent mixing is not required for planar beaches, but it is required for barred beaches to describe the longshore currents inside the surf zone. The mean value of the bed shear stress coefficient for the present longshore current data is 0.006 and the mean lateral mixing coefficient is 0.006.

## TABLE OF CONTENTS

## LIST OF TABLES

## LIST OF FIGURES

## LIST OF SYMBOLS AND ABBREVIATIONS

| SYMBOL | UNITS | NAME / DESCRIPTION |
|---|---|---|
| $\rho$ | $gram/cm^3$ | Water Density |
| g | $cm/\ sec^2$ | Gravity |
| B | dimensionless | Amount of Foam Of a Breaking Wave |
| $\gamma$ | dimensionless | Proportionality Coefficient |
| BG | $B^3/\gamma^2$ | Combined Model Parameter |
| $c_f$ | dimensionless | Bed Shear Stress Coefficient |
| $v$ | $cm^2/\ sec$ | Eddy Viscosity Coefficient |
| N | dimensionless | Lateral Mixing Coefficient |
| $\theta$ | degrees | Angle of Wave Incidence |
| $\eta$ | dimensionless | Sea Surface Elevation |
| $\tan \beta$ | dimensionless | Mean Beach Slope |
| f | hertz | Frequency |
| $H_o$ | cm | Deep Water Rms Wave Height |
| V | cm/sec | Longshore Current Velocity |
| $H_o/L_o$ | dimensionless | Deep Water Wave Steepness |
| $H_{rms}$ | cm | Rms Wave Height |
| $\xi_o$ | dimensionless | Deep Water Surf Similarity Parameter |
| $e_{rms}$ | % | Rms Error Percentage |

## ACKNOWLEDGEMENTS

This study was funded by the Naval Environmental Prediction Research Facility (NEPRF) and the Office of Naval Research. The author wishes to express his sincere appreciation to Dr. Edward B. Thornton for his guidance and constructive critisism which made this study a great learning experience. Dr. C.-S. Wu 's assistance in numerical modeling and problem discussion is gratefully acknowledged.

The author wish to express his special thanks to the entire faculty and staff of the Oceanography Department of the Naval Postgraduate School, CA for their invaluable help and understanding.

# I. INTRODUCTION

## A. BACKGROUND

The wave height and longshore current distribution inside the surf zone is a primary concern of Coastal Engineering and Naval Operations. These distributions are important for amphibious operations both at the decision making stage and during the beach assault in order to reduce the percentage of casualties. The type of landing craft to be chosen depends on the wave and current conditions in the surf zone.

As waves move from deep water to shallow water, they are transformed due to the effects of shoaling, refraction and dissipation. Shoaling results in decrease in wave length and an increase in wave height. Wave refraction results in change in wave direction. Shoaling and refraction are reasonably well defined by theory. Dissipation is due to bottom friction and wave breaking. Wave breaking is the dominant dissipative mechanism inside the surf zone. At a certain depth the waves become unstable and break in either spilling, plunging or surging form, depending on the deep water wave steepness and the beach slope. After breaking the wave height decreases as the energy is converted into turbulence and finally lost to heat. If the waves approach the beach at an angle then they cause a longshore current parallel to the shoreline within the surf zone because of the change in the alongshore component of momentum.

The motion of water inside the surf zone is extremely complex because of the dynamic upper and lower boundaries and generally three dimensional nature of the flow. In order to overcome this complexity in the surf zone, a number of assumptions have to be made. As a consequence, the models describing wave transformation and longshore currents include empirical parameters that must be specified in the formulation. The specification of these empirical parameters requires testing the model against comprehensive experimental data.

As of today, there is no exact theoretical formulation for the wave height distribution inside the surf zone where the waves break. Therefore empirical formulations are used to specify the wave height in the surf zone. It is generally assumed that the breaking wave height in the surf zone is a linear function of the depth in the form of:

$$H = \gamma h \qquad [1]$$

in which H is the wave height, h is the water depth and $\gamma$ is the proportionality constant. This relation holds fairly well for spilling breakers. It has been shown by several investigators such as Horikawa and Kuo (1967), Nakamura, Shirashi and Sasaki (1967), Divorky, Le mehauté and Lin (1970) that this relation does not hold for plunging breakers. Although this relation does not hold for all breaker types it has been retained in most models built to predict the wave height in the surf zone (Smith and Kraus, 1988). Wu *et al.* (1985) also utilize this relation in their two dimensional model that includes the bottom friction and the nonlinear convective accelerations. The major deficiency of present day models is the inability to correctly describe wave breaking processes.

## B. OBJECTIVES

The objectives of this thesis are to test and modify the wave transformation and longshore current models being considered for application in the Tactical Environmental Support System (TESS). These models are part of the the surf forecasting software which was developed under contract by Marshall D. Earle, MEC Systems Corporation to provide the Navy with an improved Surf Forecasting capability. The basis of this model are the wave transformation and longshore current models developed by Thornton and Guza (1983), (1986). In order to make the models more operational and increase the range of applicability, an expanded data base of 74 different data sets including field and lab data are utilized. The model parameters are calculated by minimizing the error in the least square sense between the model and the data, an attempt is made to predict the model parameters.

## II. NUMERICAL MODEL

The surf forecasting model predicts the wave height and longshore current distribution across the surf zone. The feature of this model compared to most previous studies is that the waves are treated as random rather than monochromatic. The coordinate system orientation and sign convention used in the model is given in Figure 1 . The shoreline has been aligned with the y-coordinate and the x-coordinate is positive offshore. A wave orthogonal approaching the beach from southerly direction has a positive angle value $(+\theta)$ and causes positive longshore current, ie, to the right, where as a northerly wave orthogonal is just the opposite.

### A. DESCRIPTION OF WAVE TRANSFORMATION MODEL

The wave height transformation for straight and parallel contours is calculated using the energy flux balance in which the onshore spatial variation of the energy flux is balanced by the ensemble averaged dissipation due to wave breaking, $< \varepsilon_b >$ , and the frictional dissipation, $< \varepsilon_f >$ . The energy flux balance is given by:

$$\frac{\partial(EC_{gx})}{\partial x} = < \varepsilon_b > + < \varepsilon_f > \qquad [2]$$

where E is the wave energy, $C_{gx}$ is the x-component of the group velocity.

Based on analysis of field data acquired at Torrey Pines Beach, CA, it was found that the Rayleigh distribution was in good agreement with the data both outside and inside the surf zone. Therefore the wave height distribution inside the surf zone is described by the Rayleigh probability density function given by:

$$p(H) = \frac{2H}{H_{rms}^2} \exp\left( -\left(\frac{H}{H_{rms}}\right)^2 \right) \qquad [3]$$

Energy and the x-component of the group velocity are described using linear theory.

$$E = \frac{1}{8} \rho g \int_0^\infty H^2 p(H) dH = \frac{1}{8} \rho g H_{rms}^2 \qquad [4]$$

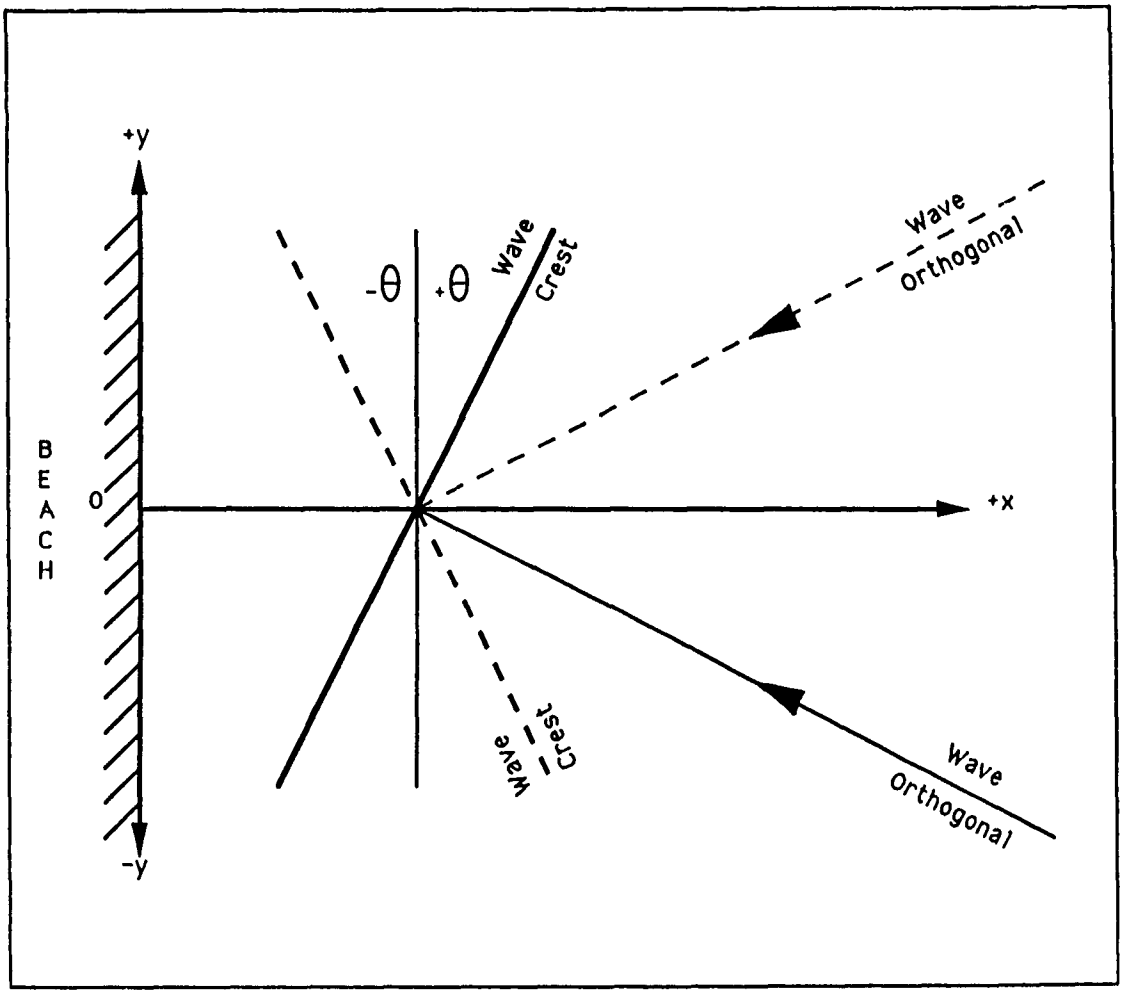


**Figure 1. Orientation of the Coordinate System and Sign Convention:** The y-axis has been aligned with the alongshore and the x-distance is positive offshore. A wave orthogonal coming from the south has a positive angle value and causes a longshore current to the right as the landing craft approaches from offshore to the beach.

$$C_{gx} = \frac{C}{2}\left(1 + \frac{2kh}{Sinh2kh}\right)\cos\bar{\theta} \qquad [5]$$

where k is the wave number associated with peak frequency $\bar{f}$, h is the water depth and $\bar{\theta}$ is the mean wave direction corresponding to the peak of the wave spectrum.

Although there are several dissipation mechanisms (frictional, percolation, sediment transport, etc. ) once the waves start to break turbulent dissipation becomes the domi-

nant dissipative mechanism. Therefore the model only includes dissipation due to wave breaking. The frictional dissipation is not included in the model because it was found that the frictional dissipation was less than 3% of the dissipation due to wave breaking. Even if this is not always true, the effect is compensated for by the B parameter in the bore dissipation mechanism. It is more reasonable to include the frictional effects in B rather than introducing new parameters. Frictional effects may become significant in the swash regions but this is not the concern of this model.

Unlike monochoromatic waves in which there is a single breaker line, the random treatment of the waves describes the larger waves to break farther offshore and the smaller waves to break closer to the shore line, which is more realistic. Across the surf zone at each point there might be broken and unbroken waves at the same time. The model calculates the breaking wave dissipation utilizing the periodic bore formulation as suggested by LeMehauté(1962). The bore dissipation mechanism as applied only to the breaking waves is formulated as follows :

$$\varepsilon_{bore} = \frac{1}{4}\rho g \frac{(h_2 - h_1)^3}{h_1 h_2} Q \simeq \frac{1}{4}\rho g \frac{(BH)^3}{h^2} Q \qquad [6]$$

where $\rho$ is the water density, g is the gravitational acceleration, $h_2$ is ( h + $\eta$ ) , $h_1$ is ( h - $\eta$ ) , $\eta$ is the surface elevation, h is the mean water depth and Q is the volume discharge across the bore. Measurements done on a gently sloping (1:40) beach show that the classical periodic bore formulation underestimates the dissipation by 30% to 50% (Stive 1983). The under-estimation is compensated for by adjusting the value of the parameter B which describes the amount of foam on the crest of a wave (see Figure 2). There are several formulations suggested for the volume discharge across the bore. The description by Hwang *et al.* (1970 ) is used in the model,

$$Q = \frac{Ch}{L} \qquad [7]$$

where C is the wave speed, L is the wave length and h is the mean water depth.

In order to find the percentage of waves that are breaking, the probability density function is simply multiplied by a weighting funtion.

$$P_b(H) = W(H)p(H) \qquad [8]$$

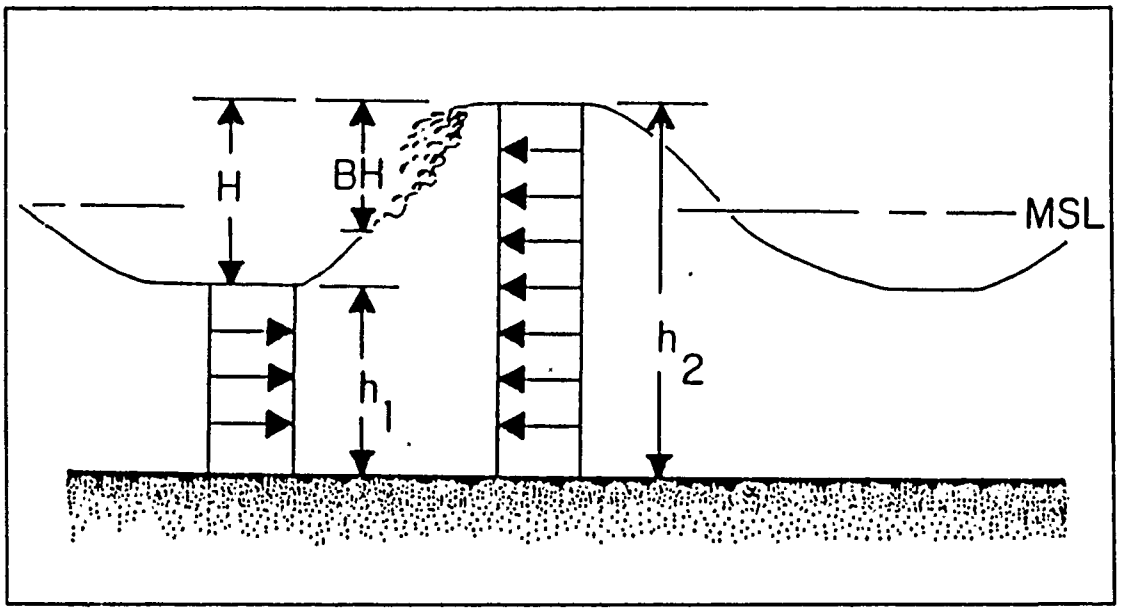


**Figure 2. Sketch of the Periodic Bore Formulation:** H is the wave height, h is the mean water level, $h_1$ is the water depth below wave trough, $h_2$ is the surface elevation measured from the bottom. B is the amount of foam over the crest of a breaking wave.

Note that $P_b(H)$, is not a pdf but a percentage. In order to distinguish the percentage of the waves that are breaking, the following empirical weighing function which fits the observations is used (Thornton and Guza, 1983)

$$W(H) = \left(\frac{H_{RMS}}{\gamma h}\right)^n \left[1 - \exp\left(-\left(\frac{H}{\gamma h}\right)^2\right)\right] \quad \leq 1 \qquad [9]$$

It was found by the same authors that a value of $\gamma = .40$ and $n = 2$ gave the best fit to the data.

The average rate of energy dissipation is found by adding up the dissipation for each breaking wave calculated using the formula

$$\varepsilon_{bore} = \frac{\tilde{f}}{4} \rho g \frac{(BH)^3}{h} \qquad [10]$$

Then this sum is divided by the total number of waves both broken and unbroken. In other words the average rate of energy dissipation is calculated by multiplying the dissi-

pation for a single broken wave height H by the probability of wave breaking at each height, as given by $P_b(H)$. For the ensemble

$$<\varepsilon_b> = \frac{B^3}{4}\rho g\frac{\bar{f}}{h}\int_0^\infty H^3 P_b(H)dH \qquad [11]$$

Substituting (10) the bore dissipation is given by :

$$<\varepsilon_b> = 3\frac{\sqrt{\pi}}{16}\rho g\bar{f}B^3\frac{H_{RMS}^5}{\gamma^2 h^3}\left[1-\frac{1}{\left(1+\frac{H_{RMS}}{\gamma h^2}\right)^{\frac{5}{2}}}\right] \qquad [12]$$

## B. DESCRIPTION OF THE LONGSHORE CURRENT MODEL

Most of the longshore current models for straight and parallel contour beaches are based on an alongshore momentum balance. Assuming steady state, the alongshore momentum balance is given:

$$\frac{\partial \tilde{S}_{yx}}{\partial x}+\frac{\partial S'_{yx}}{\partial x}=-\tau_y^b+\tau_y^\eta \qquad [13]$$

in which the first term on the left hand side is the wave induced momentum flux, or radiation stress gradient and the second term is the lateral transfer of turbulent momentum. On right hand side of the equation, are the bottom shear and surface wind stresses in the alongshore direction.

The wave induced radiation stress due to gravity waves, first introduced by Longuet-Higgins and Steward (1964), is utilized to express the change in momentum due to waves. Thornton and Guza (1983) using linear theory and the energy flux equation(2) showed that the wave induced radiation stress gradient may be expressed as

$$\frac{\partial \tilde{S}_{yx}}{\partial x}=\frac{\sin\theta_o}{C_o}\frac{\partial}{\partial x}(EC_g\cos\theta)=\frac{\sin\theta_o}{C_o}<\varepsilon_b> \qquad [14]$$

Neglecting the surface wind stress in the alongshore direction and substituting equation (12), the alongshore momentum equation becomes:

$$-\frac{\sin\theta_o}{C_o}<\varepsilon_b>=-\frac{dS'_{yx}}{dx}-\tau_y^b \qquad [15]$$

The tangential bottom stress $\tau_y^b$ for small angle of incidence and weak mean longshore current can be approximated ( Longuet-Higgins (1970a,b) ) :

$$\tau_y^b=\rho c_f\left|\bar{\vec{u}}\right|V \qquad [16]$$

in which $c_f$ is the bottom shear stress coefficient, $\left|\bar{\vec{u}}\right|$ is the mean water particle velocity magnitude and V is the mean longshore current. Thornton and Guza (1983) calculated the mean water particle velocity magnitude as :

$$\left|\bar{\vec{u}}\right|=\frac{1}{2}\sqrt{\left(\frac{g}{h}\right)}\left[\frac{\sqrt{\pi}}{2}H_{rms}\right]\left(\frac{2}{\pi}\right) \qquad [17]$$

The lateral turbulent mixing term $S'_{yx}$ is the vertically integrated Reynold's stress. Since the functional form of this stress is not known, it is usually parameterized utilizing an eddy viscosity coefficient $\nu$ :

$$S'_{yx}=\overline{\int_{-h}^{\eta}\rho u'v'dz}=-\rho\nu h\frac{dV}{dx} \qquad [18]$$

The eddy viscosity formulation by Longuet-Higgins (1970b), which spatially decrease from offshore to onshore, is used in the model :

$$\nu=N|x|\sqrt{gh} \qquad [19]$$

where N is an adjustable coefficient and based on dimensional analysis has an approximate range of $0\le N\le 0.016$ .

If the lateral transfer of momentum is not negligible and is to be included, then the alongshore momentum balance equation is a second order ordinary differential equation. In this case, the gradient of this term is given by:

$$\frac{dS'_{yx}}{dx}=-\rho N\sqrt{g}\,\frac{d}{dx}\left[|x|h^{3/2}\frac{dV}{dx}\right] \qquad [20]$$

Taking the derivatives,

$$\frac{dS'_{yx}}{dx} = -\rho N\sqrt{g}\left[\left(h^{3/2}\frac{dV}{dx}\right)+\left(\frac{3}{2}\sqrt{h}\,x\frac{dh}{dx}\frac{dV}{dx}\right)+\left(h^{3/2}x\frac{d^2V}{dx^2}\right)\right] \quad [21]$$

Substituting back into the steady state alongshore momentum equation, we have:

$$-\frac{\sin\theta_o}{C_o}<\varepsilon_b> =$$

$$\rho N\sqrt{g}\left[h^{3/2}\frac{dV}{dx}+\frac{3}{2}\sqrt{h}\,x\frac{dh}{dx}\frac{dV}{dx}+h^{3/2}x\frac{d^2V}{dx^2}\right]-\rho c_f\left|\bar{\vec{u}}\right|V \quad [22]$$

Grouping the terms, we end up with the following second order differential equation.

$$\frac{d^2V}{dx^2} = \left[\frac{c_f\left|\bar{\vec{u}}\right|}{N\sqrt{g}\,xh^{3/2}}\right]V-\left[\frac{1+\frac{3}{2h}\frac{dh}{dx}x}{x}\right]\frac{dV}{dx}+$$

$$\left[\frac{\left(-\frac{\sin\theta_o}{C_o}<\varepsilon_b>\right)}{\left(\rho N\sqrt{g}\,xh^{3/2}\right)}\right] \quad [23]$$

## C. APPLICATION OF THE MODEL

### 1. Wave Height Model

To apply the wave height model, the the parameters B and $\gamma$ are combined, reducing the degree of freedom to one. The B parameter describes the amount of foam on the face of a breaking wave i.e. the intensity of wave breaking, $\gamma$ is a proportionality constant that relates the rms breaking wave height to the water depth and is slope dependent. The combined parameter is designed to reduce the number of free parameters to tune the model. The term in brackets of equation 12 in the bore dissipation equation is a correction term to the original bore dissipation formulation. Therefore when the B and $\gamma$ parameters were combined the $\gamma$ term in the brackets was assigned a typical value of 0.40. The combined parameter BG is equal to $\frac{B^3}{\gamma^2}$.

The model generated wave heights and data were compared by finding the BG value that results in the minimum root mean square error

$$e_{rms} = \sqrt{\frac{1}{n}\sum_{i=1}^{n}\frac{(H_{model} - H_{data})^2}{H_{data}^2}} \qquad [26]$$

where $H_{model}$ is the model generated wave height, $H_{data}$ is the measured wave height and n is the number of data points. The model was iterated over the combined parameter BG and the rms error was computed. The BG parameter was varied from low to high values to observe the model behavior and stability. Based on the minimum rms error, the best fit was obtained. Examples from each data set for the model fit to the wave height data are shown in Figures 9 to 14.

**2. Longshore Current Model**

The longshore current model was compared with the measured longshore currents for planar beaches and reasonable results were obtained with and without turbulent mixing. Similar comparision for barred beaches showed that the model fails to predict the longshore current over the shore side of the bar when turbulent mixing is not included. In order to improve the results, turbulent mixing parameterized by an eddy viscosity was included in the model, which increased the degree of longshore current equation to the second.

This second order differential equation (23) was solved numerically using a centered difference scheme. The equation was put in a finite difference form and a linear system of equations were obtained for the interior of the spatial domain. At the shoreline, a zero current boundary condition was assumed and the very offshore value measured in the data was used as the offshore boundary condition. The system of equations was put in a tridiagonal matrix. The tridiagonal matrix was solved by a convenient tridiagonal solver by Maron (1987). A mid value of 0.008 was assigned to the lateral mixing coefficient, $N$ , which has an approximate range of 0.0 to 0.016 and the model was iterated over the bed shear coefficient until the error between the model generated current and the data is minimized. Then with the best shear stress coefficient obtained the model was iterated over $N$ from 0.0 to .030 until the rms error was reduced. Examples of model fits of Superduck and Santa Barbara data are shown in Figure 15 and 16 respectively.

# III. DATA AND METHODS

## A. WAVE HEIGHT TRANSFORMATION

To test and modify the wave transformation model, 74 data sets were used. The data consisted of both laboratory and field data. These data provided many different wave conditions from the long period, low steepness Pacific swell to steeper Atlantic and North Sea storm waves. The experiments were conducted over various bottom profiles including both planar and barred beaches. The data sets are described below. The data sets are named after either the site of the data or the person that acquired the data. In the tables that describe the data, tan$\beta$ is the mean beach slope, f is the peak frequency in hertz, $H_{rms}$ is the root mean square wave height, $\frac{H_o}{L_o}$ is the deep water wave steepness, $\xi_o$ is the deep water surf similarity parameter, BG is the combined model parameter and $e_{rms}$ is the rms error percentage between the model generated wave height and the data.

The deep water surf similarity parameter

$$\xi_o = \frac{\tan\beta}{\sqrt{\frac{H_o}{L_o}}} \qquad [27]$$

was calculated for each data set in which $H_o$ is the deep water wave height, $L_o$ is the deep water wave length and tan$\beta$ is the mean beach slope (Battjes 1974). The deep water wave height was calculated from the measured wave height in shallower water using the linear wave theory shoaling coefficient corresponding to the the peak frequency. Similarly, the deep water wave length was calculated from the peak frequency using linear wave theory.

### 1. Torrey Pines ( NSTS )Data

Torrey Pines wave height data were acquired as part of the Nearshore Sediment Transport Study (NSTS) at Torrey Pines Beach, CA, during November 1978. The beach was gently sloping, near planar and homogeneous in alongshore direction. Shadowing effects of the offshore islands and refraction limits the angle of wave incidence in the surf zone to a narrow band of less than $\mp$ 15 degrees and usually much less. The winds during the experiment were light and variable during the experiment. An extensive array

of instruments was deployed to study the nearshore wave dynamics. The sensors used in this study were 11 Marsh-McBirney electromagnetic current meters, four Stathem pressure transducers and four resistance wire wave staff. The wave heights were determined by the zero-up crossing method, in which the wave height is defined as the difference between maximum and minimum within two consecutive zero-up crossings. The data were filtered to include only the wind wave band of frequencies between 0.05 and 0.3 Hz . The data are described in Table 1. Details of the experiment are given in Thornton and Guza (1983).

**Table 1. TORREY PINES WAVE HEIGHT DATA**

| CASE | DATA TYPE | tan$\beta$ | f (Hz) | $H_{rms}$ (cm.) | $H_0/L_0$ | $\xi_o$ | BG | $e_{rms}$ (%) |
|---|---|---|---|---|---|---|---|---|
| Nov 04 | Field | .021 | .063 | 35.0 | .0007 | .78 | 11.8 | 7.1 |
| Nov 10 | Field | .021 | .055 | 56.0 | .0008 | .72 | 13.6 | 10.9 |
| Nov 12 | Field | .021 | .077 | 81.0 | .0027 | .39 | 7.6 | 4.0 |
| Nov 17 | Field | .023 | .069 | 47.1 | .0011 | .69 | 13.8 | 7.3 |
| Nov 18 | Field | .023 | .069 | 53.0 | .0012 | .65 | 11.2 | 3.8 |
| Nov 20 | Field | .023 | .063 | 56.2 | .0011 | .71 | 12.2 | 5.9 |

**2. Santa Barbara (NSTS) Data**

The Santa Barbara data (Table 2) were acquired during the second NSTS experiment conducted at Leadbetter Beach from 30 January to 23 February 1980. The site was selected because the waves are homogeneous in the alongshore direction and the bottom contours are relatively straight and parallel. The Leadbetter Beach is composed of wellsorted fine to medium size sand. The mean nearshore slope varied between .03 to .06 during the experiment. The shoreline has an unusual east-west orientation along a predominantly north-south coast. The open ocean waves are limited to a narrow window of approach -9 degrees to +9 degrees centered at 249 degrees. Therefore the waves from the open ocean were directionally narrow banded swell arriving at relatively large angles of about 10 degrees to the shoreline. Instrumentation included 24 Marsh-McBirney electromagnetic current meters and 14 pressure sensors. The experiment is described in detail in Thornton and Guza (1986).

**3. Battjes and Stive (1985) Data**

The first three cases ( Table 3 ) are lab data that were acquired in a wave flume using mechanically generated random waves. The bottom profiles include a schematized

**Table 2. SANTA BARBARA WAVE HEIGHT DATA**

| CASE | DATA TYPE | tan$\beta$ | f (Hz) | $H_{rms}$ (cm.) | $H_0/L_0$ | $\xi_o$ | BG | $e_{rms}$ (%) |
|---|---|---|---|---|---|---|---|---|
| Feb 02 | Field | .059 | .063 | 32.4 | .0010 | 1.8 | 5.6 | 10.2 |
| Feb 03 | Field | .044 | .070 | 54.6 | .0023 | .9 | 5.2 | 12.0 |
| Feb 04 | Field | .038 | .070 | 56.0 | .0024 | .7 | 6.6 | 7.8 |
| Feb 05 | Field | .035 | .078 | 45.1 | .0023 | .7 | 4.8 | 7.5 |
| Feb 06 | Field | .033 | .090 | 26.4 | .0017 | .8 | 8.4 | 8.8 |

bar profile and a plane slope in concrete (Case 5 and Case 10). Case 15 has a profile with bar and trough on sand. All of the lab wave height data were measured by means of parallel wire conductivity wave gages.

Case 18 data is field data acquired on a beach near Egmond City, The Netherlands. The field site was chosen to have more or less statistically uniform conditions alongshore and normal wave incidence. These field data were acquired under stormy conditions during which the incident rms wave height was 2.8 meters. It was noted that the wind influence was negligible. The $H_{rms}$ was calculated from the surface elevation time series assuming that the surface elevation is a narrow band Gaussian process, which appears to be in good agreement with observations ( Thornton and Guza 1983). The rms wave height is related to the standard deviation, $\sigma$, of the surface elevation by

$$H_{rms} = \sqrt{8}\,\sigma \qquad [28]$$

**Table 3. BATTJES AND STIVE WAVE HEIGHT DATA**

| CASE | DATA TYPE | tan$\beta$ | f (Hz) | $H_{rms}$ (cm.) | $H_0/L_0$ | $\xi_o$ | BG | $e_{rms}$ (%) |
|---|---|---|---|---|---|---|---|---|
| 5 | Lab | .034 | .443 | 11.8 | .016 | .27 | 3.1 | 8.7 |
| 10 | Lab | .025 | .663 | 13.6 | .038 | .13 | 2.0 | 15.7 |
| 15 | Lab | .012 | .557 | 13.2 | .029 | .07 | 1.0 | 7.5 |
| 18 | Field | .010 | .115 | 278 | .026 | .07 | 2.2 | 12.6 |

### 4. Superduck (1986) Data

The Superduck data (Table 4) were acquired during the one month long experiment held by the U.S. Army Corps of Engineers at the Field Research Facility in Duck, N.C. in October 1986. The experiment was called Superduck. The site of the experiment is along an extensive barrier island formation known as North Carolina's Outer Banks. There are no major structures along the shoreline. The beach has a mean foreshore slope of 1:10, usually a single bar formation and a mean slope of 1:100 offshore the bar. Extensive bathymetric data were acquired using the Coastal Research Amphibious Buggy (CRAB) so that the wave height and longshore currents could be processed with accurate and detailed bathymetry data. The waves and currents were measured using a pressure sensor and a vertical array of three Marsh-McBirney current meters mounted on a moveable sled. The details of the data can be found in Whitford and Thornton (1989).

**Table 4. SUPERDUCK WAVE HEIGHT DATA**

| CASE | DATA TYPE | $\tan\beta$ | f (Hz) | $H_{rms}$ (cm.) | $H_0/L_0$ | $\xi_o$ | BG | $e_{rms}$ (%) |
|---|---|---|---|---|---|---|---|---|
| Oct 15 | Field | .037 | .160 | 92.0 | .0207 | .25 | 3.4 | 9.7 |
| Oct 16 | Field | .049 | .190 | 98.1 | .0239 | .26 | 2.8 | 13.4 |
| Oct 17 | Field | .041 | .190 | 72.0 | .0175 | .31 | 9.4 | 8.1 |
| Oct 18 | Field | .038 | .190 | 93.0 | .0226 | .25 | 5.2 | 8.2 |

### 5. Vincent (1984) Data

The Vincent data (Table 5) were acquired from a series of experiments done at the Coastal Engineering Research Center (CERC) in a wave tank of 44 meters long, 0.6 meters wide and a water depth of 0.6 meters. At one end of the tank was a smooth concrete ramp with a slope of 1:30 . A random wave generator was used to generate waves. The wave height data were measured using nine resistance wave gauges (Vincent, 1984).

Table 5. VINCENT WAVE HEIGHT DATA

| CASE | DATA TYPE | tan$\beta$ | f (Hz) | $H_{rms}$ (cm.) | $H_0/L_0$ | $\xi_o$ | BG | $e_{rms}$ (%) |
|---|---|---|---|---|---|---|---|---|
| 1058 | Lab | 1:30 | .885 | 8.6 | .0456 | .16 | .6 | 10.8 |
| 1116 | Lab | 1:30 | .763 | 11.2 | .0452 | .16 | .8 | 5.9 |
| 1132 | Lab | 1:30 | .769 | 13.1 | .0538 | 14 | .8 | 7.6 |
| 1148 | Lab | 1:30 | .671 | 14.6 | .0461 | .17 | .8 | 5.0 |
| 1206 | Lab | 1:30 | .671 | 15.7 | .0499 | .16 | 3 | 6.0 |
| 1509 | Lab | 1:30 | .403 | 6.2 | .0065 | .41 | 2.6 | 2.9 |
| 1526 | Lab | 1:30 | .403 | 9.3 | .0098 | .34 | 2.2 | 6.6 |
| 1604 | Lab | 1:30 | .403 | 12.1 | .0128 | .30 | 1.6 | 6.9 |
| 1623 | Lab | 1:30 | .403 | 14.5 | .0153 | .27 | 1.8 | 5.6 |
| 1638 | Lab | 1:30 | .403 | 15.2 | .0160 | .27 | 1.6 | 7.5 |

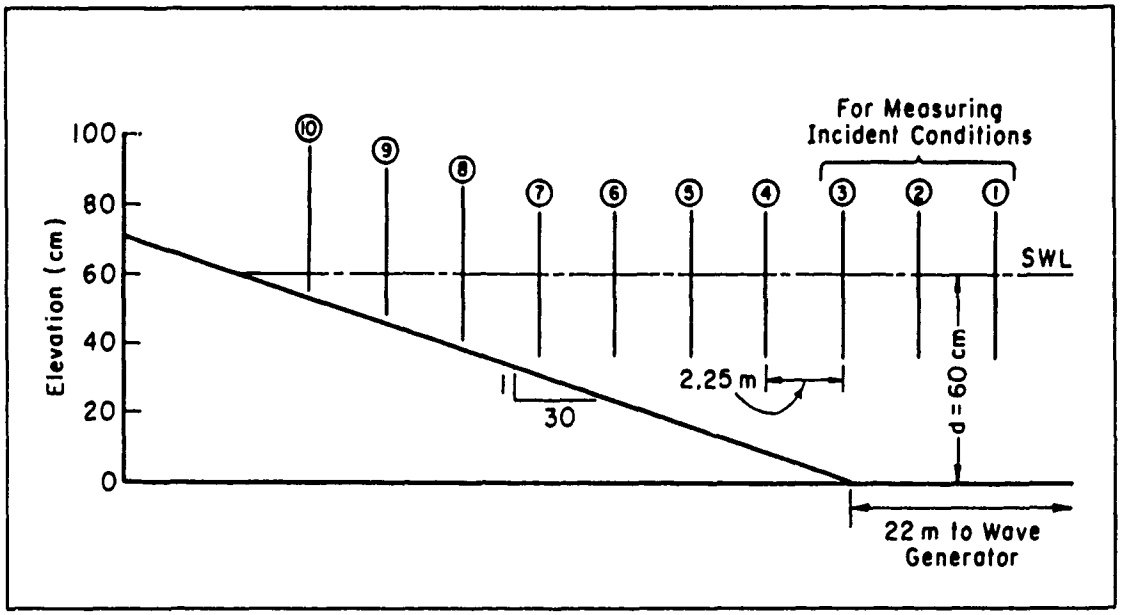


**Figure 3. Setup In CERC Wave Tank:** Ten gages were placed three of them were located over the horizontal bottom and seven of them over the 1:30 slope.

## 6. CERC (1983) Data

Wave height data (Tables 6 and 7) were acquired in Coastal Engineering Research Center (CERC)'s wave tank. The tank was 0.9 meters high, 0.4 meters wide and 45.7 meters long. The setup of this tank was designed to obtain data on the shoaling and breaking random waves. Ten parallel resistance wire wave gages were used. Three of them were located over the horizontal bottom of the tank and seven of them over the 1:30 concrete slope ( Figure 3 ).

**Table 6. CERC WAVE HEIGHT DATA ( PART I )**

| CASE | DATA TYPE | tan$\beta$ | f (Hz) | $H_{rms}$ (cm.) | $H_0/L_0$ | $\xi_o$ | BG | $\epsilon_{rms}$ (%) |
|---|---|---|---|---|---|---|---|---|
| 30 | Lab | 1:30 | .699 | 6.1 | .0199 | .24 | 4.1 | 6.7 |
| 31 | Lab | 1:30 | .758 | 6.3 | .0241 | .21 | 4.1 | 6.7 |
| 32 | Lab | 1:30 | .667 | 6.7 | .0204 | .23 | 2.7 | 2.2 |
| 33 | Lab | 1:30 | .505 | 3.6 | .0064 | .42 | 3.3 | 5.7 |
| 34 | Lab | 1:30 | .757 | 6.8 | .0261 | .21 | 2.1 | 1.9 |
| 35 | Lab | 1:30 | .684 | 3.8 | .0121 | .30 | 3.5 | 5.0 |
| 36 | Lab | 1:30 | .684 | 7.6 | .0242 | .21 | 2.2 | 1.9 |
| 37 | Lab | 1:30 | .800 | 6.4 | .0270 | .20 | 2.4 | 2.4 |
| 38 | Lab | 1:30 | .769 | 6.5 | .0259 | .21 | 2.3 | 2.1 |
| 39 | Lab | 1:30 | .684 | 4.4 | .0139 | .28 | 3.6 | 5.1 |
| 40 | Lab | 1:30 | .657 | 6.7 | .0200 | .24 | 2.7 | 3.0 |
| 41 | Lab | 1:30 | .564 | 9.0 | .0201 | .24 | 2.1 | 2.0 |
| 42 | Lab | 1:30 | .558 | 4.4 | .0096 | .34 | 3.9 | 4.6 |
| 43 | Lab | 1:30 | .284 | 4.7 | .0023 | .69 | 5.0 | 3.5 |
| 44 | Lab | 1:30 | .289 | 9.8 | .0051 | .47 | 2.6 | 6.9 |
| 45 | Lab | 1:30 | .598 | 6.7 | .0167 | .26 | 2.6 | 3.4 |
| 46 | Lab | 1:30 | .320 | 7.4 | .0049 | .48 | 3.6 | 6.0 |
| 47 | Lab | 1:30 | .316 | 5.8 | .0037 | .54 | 4.7 | 5.1 |
| 48 | Lab | 1:30 | .452 | 5.7 | .0081 | .37 | 3.9 | 4.3 |
| 49 | Lab | 1:30 | .680 | 6.5 | .0024 | .23 | 2.2 | 2.1 |
| 50 | Lab | 1:30 | .680 | 6.5 | .0204 | .23 | 2.1 | 2.1 |
| 51 | Lab | 1:30 | .598 | 6.7 | .0167 | .26 | 2.7 | 3.4 |

**Table 7. CERC WAVE HEIGHT DATA ( PART II )**

| CASE | DATA TYPE | tan$\beta$ | f (Hz) | $H_{rms}$ (cm.) | $H_0/L_0$ | $\xi_o$ | BG | $e_{rms}$ (%) |
|---|---|---|---|---|---|---|---|---|
| 52 | Lab | 1:30 | .452 | 5.8 | .0082 | .37 | 3.9 | 4.3 |
| 53 | Lab | 1:30 | .680 | 6.5 | .0204 | .23 | 2.2 | 2.1 |
| 54 | Lab | 1:30 | .680 | 6.5 | .0204 | .23 | 2.1 | 2.2 |
| 55 | Lab | 1:30 | .598 | 6.7 | .0167 | .26 | 2.7 | 3.6 |
| 56 | Lab | 1:30 | .543 | 7.1 | .0147 | .27 | 3.3 | 1.8 |
| 57 | Lab | 1:30 | .239 | 7.7 | .0025 | .66 | 4.7 | 4.1 |
| 58 | Lab | 1:30 | .234 | 7.7 | .0024 | .68 | 4.0 | 5.6 |
| 59 | Lab | 1:30 | .461 | 5.7 | .0085 | .36 | 4.4 | 3.0 |
| 60 | Lab | 1:30 | .370 | 5.7 | .0052 | .46 | 4.8 | 1.5 |
| 61 | Lab | 1:30 | .384 | 3.8 | .0037 | .54 | 7.0 | 2.8 |
| 62 | Lab | 1:30 | .384 | 3.8 | .0037 | .54 | 7.0 | 2.6 |
| 63 | Lab | 1:30 | .543 | 7.2 | .0148 | .27 | 3.4 | 2.0 |
| 64 | Lab | 1:30 | .680 | 9.8 | .0308 | .19 | 2.0 | 3.4 |
| 6. | Lab | 1:30 | .680 | 9.8 | .0308 | .19 | 1.9 | 3.3 |
| 66 | Lab | 1:30 | .598 | 9.8 | .0243 | .21 | 2.4 | 1.9 |
| 67 | Lab | 1:3' | .598 | 9.9 | .0247 | .21 | 2.3 | 1.5 |
| 68 | Lab | 1:[illegible] | .281 | 8.6 | .0042 | .52 | 3.3 | 4.7 |
| 69 | Lab | 1:30 | .277 | 8.6 | .0040 | .53 | 3.3 | 3.6 |
| 70 | Lab | 1:30 | .294 | 10.2 | .0056 | .45 | 3.2 | 3.9 |
| 71 | Lab | 1:30 | .649 | 5.4 | .0157 | .27 | 3.7 | 3.8 |
| 72 | Lab | 1:30 | .667 | 6.1 | .0187 | .24 | 3.3 | 2.8 |
| 73 | Lab | 1:30 | .598 | 5.6 | .0140 | .28 | 3.9 | 3.0 |
| 74 | Lab | 1:30 | .602 | 5.9 | .0148 | .27 | 3.7 | 3.0 |

## B. LONGSHORE CURRENTS

The longshore current model described in Chapter 2 is applied to the Santa Barbara and Superduck data sets. These are the only high quality longshore current data available acquired on a homogeneous alongshore bathymetry with adequate measure of directional wave forcing. The Santa Barbara beach profiles were almost planar while the Superduck profiles were barred. Of the combined two months of data collection, five cases from Santa Barbara and four cases from Superduck were selected for comparision.

Since the longshore currents are induced by the wind waves, simultaneous measurements of the wave field and longshore current measurements is essential. This requirement was satisfied in the data sets. In the Tables 8 and 9 describing the longshore currents, $c_f$ is the bed shear stress coefficient, N is the lateral mixing coefficient, f is the frequency in hertz, $H_{rms}$ is the the rms wave height, $\frac{H_o}{L_o}$ is the deep water wave steepness, $\xi_o$ is the deep water surf similarity parameter, $e_{rms}$ is the rms error percentage between the model generated longshore current and the data.

**Table 8. SANTA BARBARA LONGSHORE CURRENT DATA**

| CASE | $c_f$ | N | f (Hz) | $H_{rms}$ (cm.) | $H_0/L_0$ | $\theta$ | $\xi_o$ | $e_{rms}$ (%) |
|---|---|---|---|---|---|---|---|---|
| Feb 02 | .0085 | .0160 | .063 | 32.4 | .0010 | 6.4 | 1.8 | 50.0 |
| Feb 03 | .0090 | .0190 | .070 | 54.6 | .0023 | 7.8 | .90 | 55.5 |
| Feb 04 | .0090 | .0001 | .070 | 56.0 | .0024 | 9.0 | .77 | 27.9 |
| Feb 05 | .0060 | .0010 | .078 | 45.1 | .0023 | 8.4 | .73 | 22.1 |
| Feb 06 | .0080 | .0020 | .090 | 26.4 | .0017 | 8.3 | .79 | 31.0 |

**Table 9. SUPERDUCK LONGSHORE CURRENT DATA**

| CASE | $c_f$ | N | f (Hz) | $H_0$ (cm.) | $H_0/L_0$ | $\theta$ | $\xi_o$ | $e_{rms}$ (%) |
|---|---|---|---|---|---|---|---|---|
| Oct 15 | .0025 | .0010 | .160 | 92.0 | .0207 | 9.1 | .25 | 5.9 |
| Oct 16 | .0035 | .0030 | .190 | 98.1 | .0239 | 14.7 | .26 | 4.5 |
| Oct 17 | .0065 | .0001 | .190 | 72.0 | .0175 | 6.3 | .31 | 7.1 |
| Oct 18 | .0005 | .0070 | .190 | 93.0 | .0220 | 11.8 | .25 | 17.7 |

# IV. DISCUSSION

The wave transformation model was applied to 74 different data sets. The very offshore wave height and direction measured were used as an input to the model. The model is not very sensitive to the exact orientation of waves to the shoreline since the group speed computations involves the cosine of the angle of wave incidence and the cosine of a small angle is not significantly different from one. Therefore exact wave orientation is not required and the error due to wave orientation is expected to be small.

The data sets and the profiles were compiled and the model was iterated over the BG parameter to reduce the root mean square error percentages in the least square sense. A fully developed bore would be expected to have a B value of 1 and since the typical proportionality constant $\gamma$ for Rayleigh distribution is about 0.4, the combined parameter BG for a fully developped bore would be equal to 6.25. The statistics of the BG parameter for the whole 74 data sets were computed. A mean of BG parameter of 4 with a standard deviation of 2.9 was obtained for all the data sets.

Model sensitivity to the choice of the $\gamma$ parameter was investigated by Gill (1985). He varied the $\gamma$ parameter from 0.35 to 0.55 and found that the error increase was less than 8-10%. In the same manner, the B parameter was iterated from 0.9 to 1.7 and it was found that the increase in rms error was less than 10-12%. Similar type of investigations were done by Thornton and Guza (1983) for Torrey Pines data set and it was found that varying the B parameter $\mp$ 25% resulted in an increase of rms error less than 10%.

The combined parameter BG is plotted against the rms error in Figure 5, and it is seen that changing the BG parameter one standard deviation either side of the mean causes an increase in rms error of less than 9% . Based on these investigations it is evident that the model is not overly sensitive to the exact choice of parameters.

Relatively high values of BG parameter are required to minimize the rms error for Torrey Pines data. The Santa Barbara data had almost the same deep water steepness but didn't require as high values of BG. The difference is hypothesized due to the deficiencies of linear bore theory. For spilling type breaker the turbulence is confined to a surface layer, basically between the crest and trough of a wave. For plunging or surging type breaking the turbulence is not confined between the crest and trough, but penetrates much deeper. The actual depth h, concerning the volume discharge computation

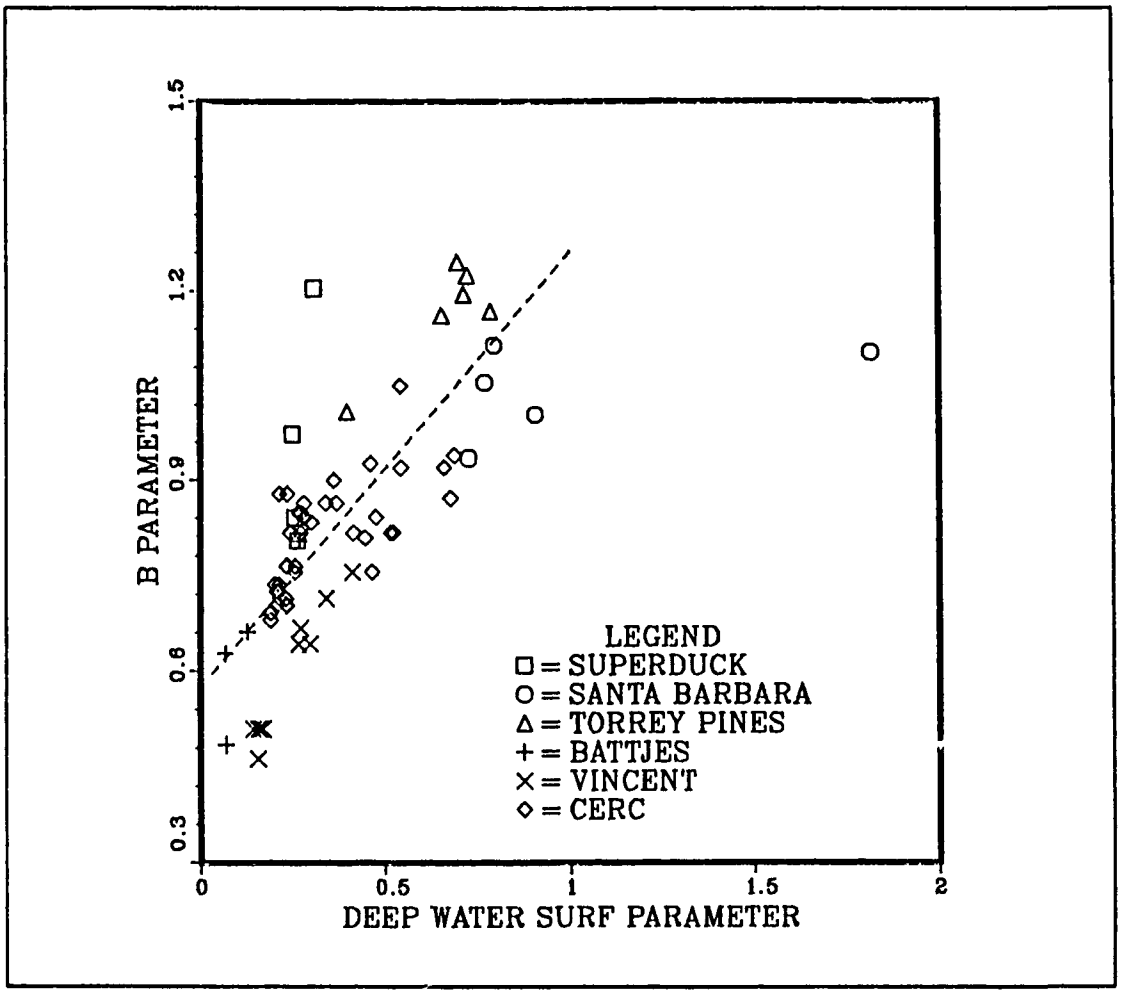


**Figure 4. Variation of B with Deep Water Surf Similarity Parameter:** The B parameter shows a linear trend with the deep water surf similarity parameter, $\xi_o$. The dashed line is the linear regression line. Notice that the B parameter values increase as the breaker type shifts from spilling to plunging ($\xi_o > 0.4$).

will be different from the mean water level as expressed by the linear bore theory. It is evident that there is deviation from the bore formulation. Although the incident wave parameters such as deep water steepness and frequency for Torrey Pines and Santa Barbara data sets are about the same, the beach slope of Santa Barbara is about twice that of Torrey Pines. This result implies that the wave breaking is a function of both deep water wave steepness ($\frac{H_o}{L_o}$) and beach slope ($\tan\beta$). Therefore the wave dissipation

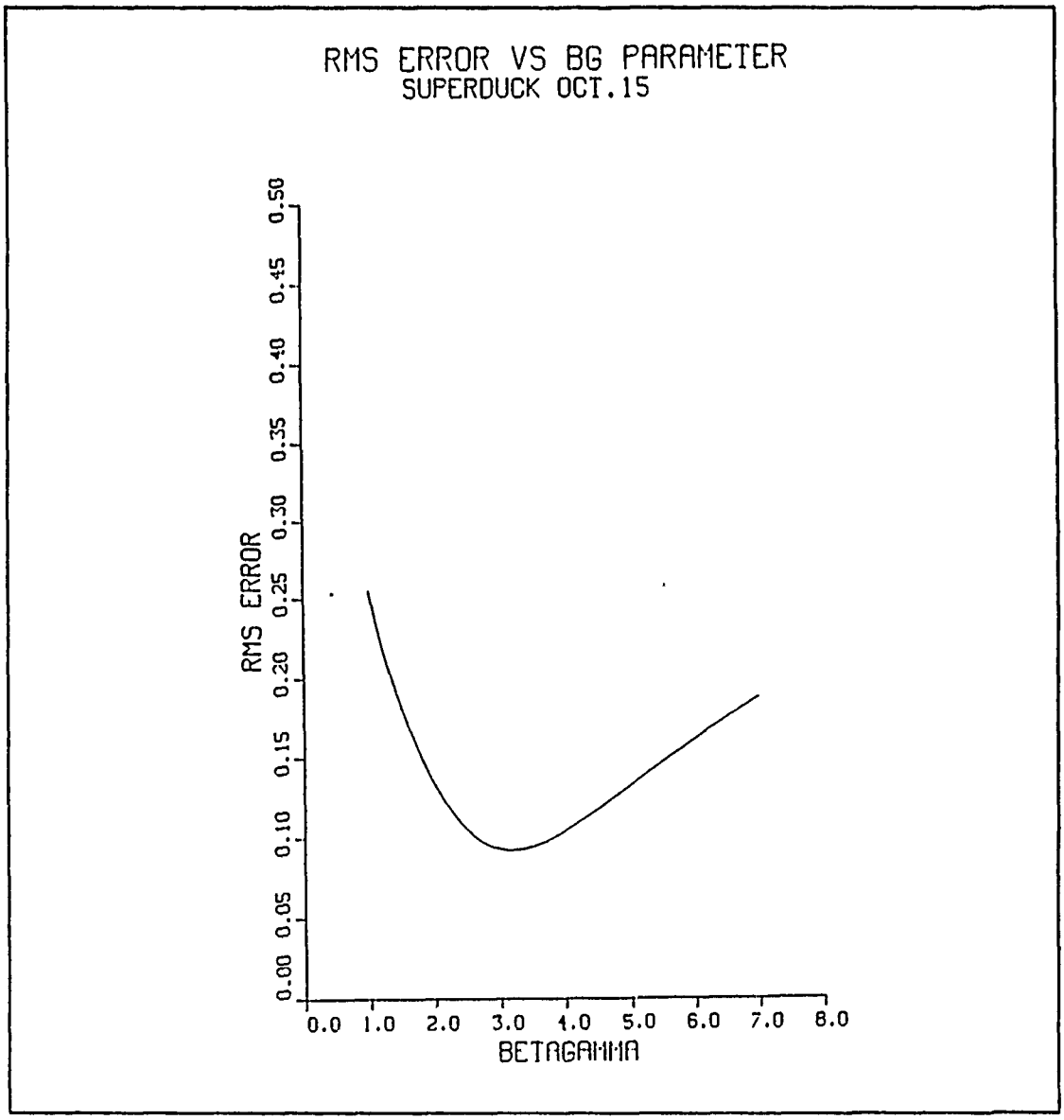


**Figure 5. Variation In Rms Error Due to Change In BG Parameter:** Changing BG (BETAGAMMA) parameter one standard deviation on either side of the mean does not increase the error greater than 9%.

rate is lower over mild slopes compared to steep slopes. The combination of plunging type breaker and the beach slope effect is thought to be responsible for high values of BG for Torrey Pines data set. This idea is confirmed when the BG parameter obtained for all cases plotted versus deep water steepness. As seen in (Figure 6), as the deep

water steepness becomes less than 0.02 the BG parameter tends to increase exponentially. For deep water steepness greater than 0.02 the BG parameter stays invariant at a value of about 2.9. The curve fitted to the individual points has the form of $y = \alpha + \frac{\beta}{x}$ where $\alpha$ is equal to 2.25 and $\beta$ is equal to 0.0085.

Using the deep water surf similarity parameter the breaker type is classified as follows (Battjes, 1974) :

| | |
|---|---|
| $\xi_o < 0.4$ | Spilling |
| $0.4 \leq \xi_o \leq 2.0$ | Plunging |
| $\xi_o > 2.0$ | Surging or Collapsing |

Most of the data sets tabulated in chapter 2 fall in the spilling range with a few of them being in the plunging range. There were no surging or collapsing type breaker. Torrey Pines and Santa Barbara (NSTS) data differ from the other data due to their low steepness, about one order of magnitude smaller than the other data sets. As a result, the breaker type based on the surf similarity parameter by Battjes (1974) suggest plunging for all cases of the NSTS data sets. Breaking intensity increases from spilling to plunging to collapsing breakers as $\xi_o$ increases. Therefore it is expected B and hence BG will be a function of $\xi_o$ and increase as $\xi_o$ increases.

The BG parameters obtained for all data sets are plotted versus deep water surf parameter and an exponential trend was observed. A curve in the form of $y = \alpha e^{\beta x}$ is fitted. Excluding one outlying data point seen in the right side of Figure 7 , it is found that $\alpha = 1.303$ and $\beta = 2.4$ fitted the data well. This curve acts in a very similar manner to the breaking wave height curves in the Shore Protection Manuel, U.S. Army Corps of Engineers (1984) in this exponentially increasing region of the curve. Utilizing this function, the model parameter can be predicted. The deep water surf parameter can be computed for a particular beach of interest and inputting this value to the fitted curve function, the BG parameter can be predicted.

The BG parameter was plotted versus the incident rms wave height. No correlation was evident. Therefore it was concluded that the model parameter is not strongly dependent on incident wave height by itself. Running all the data sets, it was observed that the model is capable of handling a small scale wave height of 6 cm lab data as well as a 278 cm large wave height measured during a stormy weather.

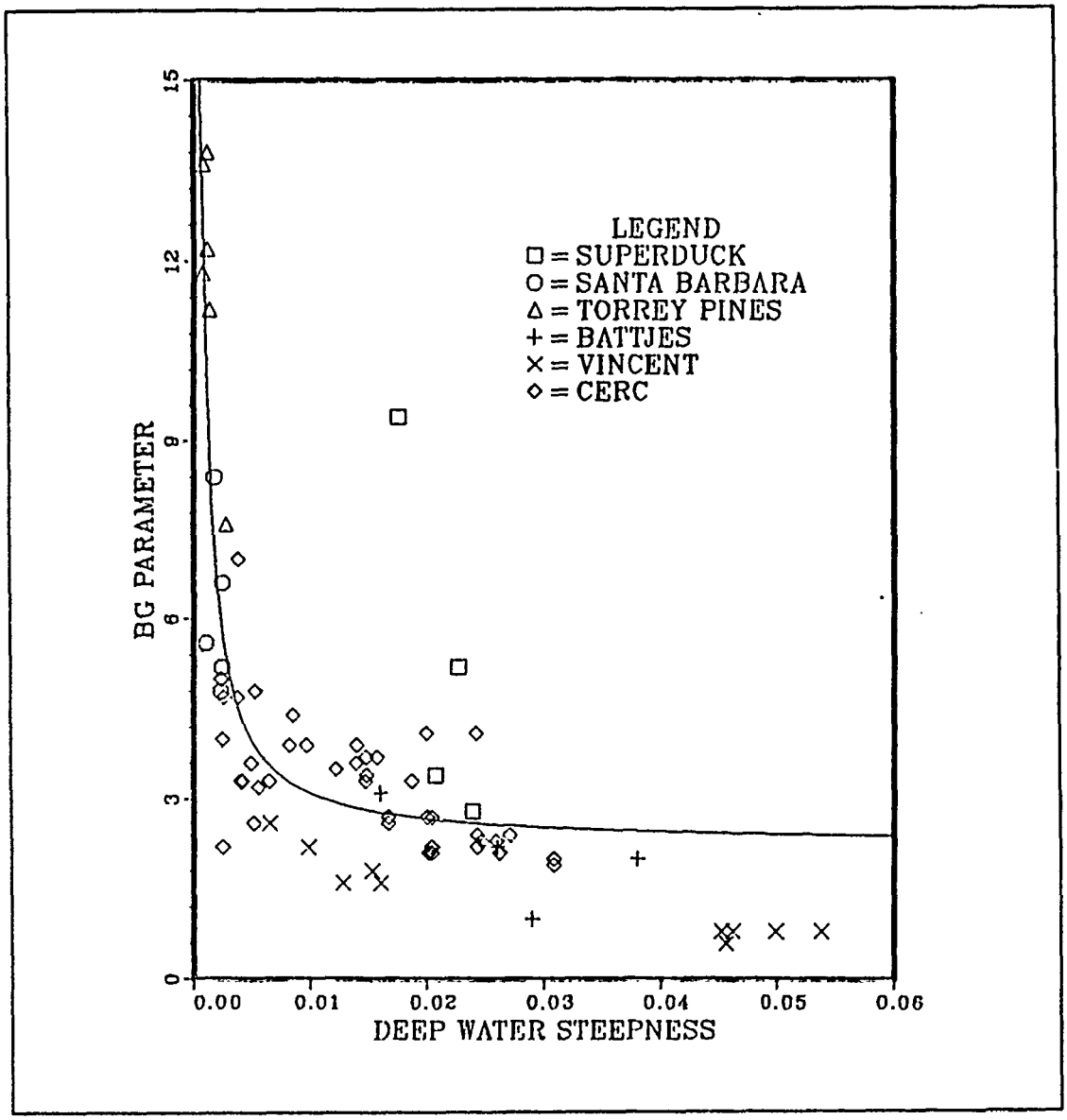


**Figure 6. BG Versus Deep Water Steepness:** The solid curve represents the curve fitted to BG values versus deep water steepness for all data sets in the form of $y = \alpha + \frac{\beta}{x}$.

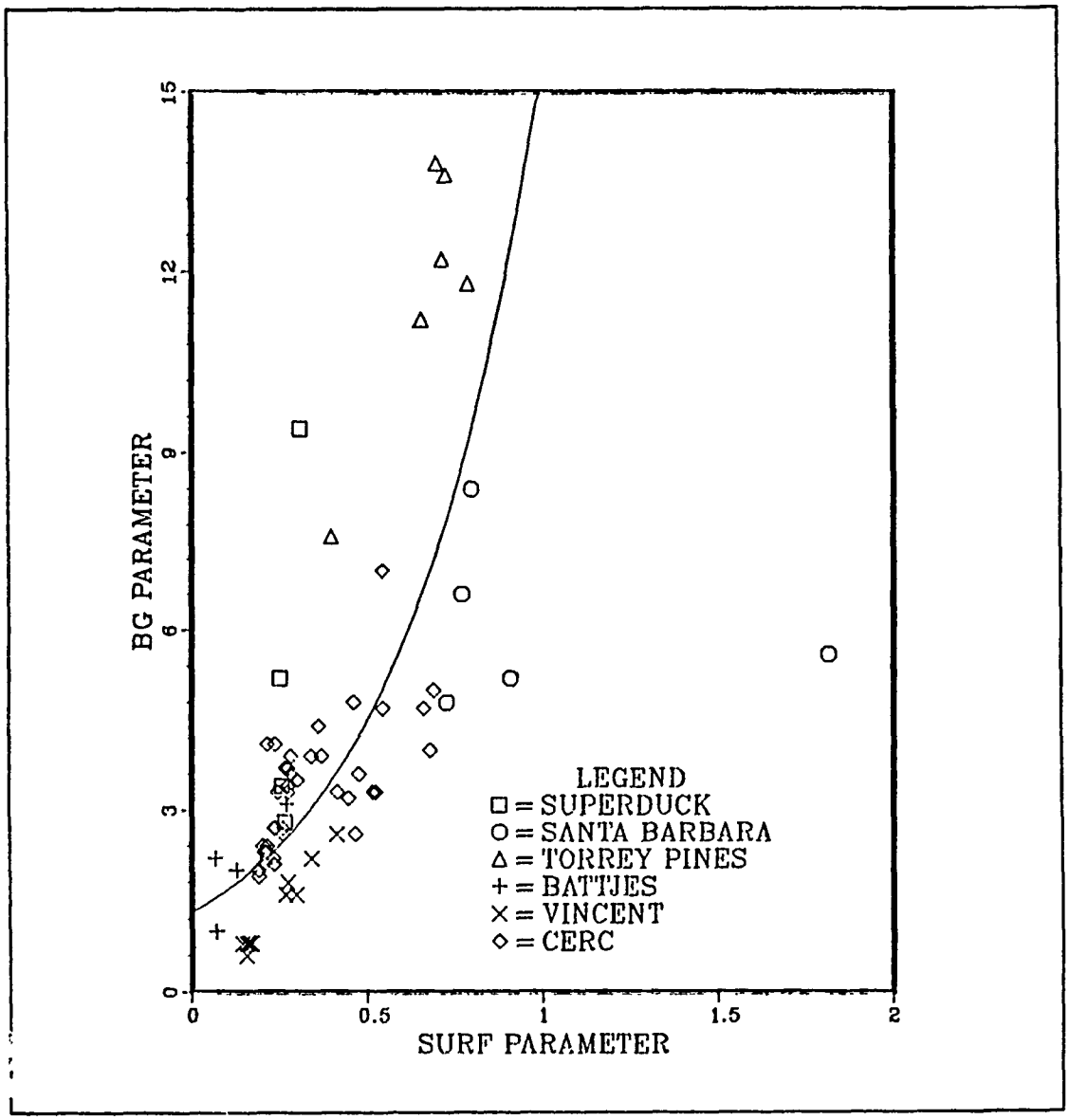


**Figure 7. BG Versus Deep Water Surf Parameter:** The solid curve represents the curve fitted to BG values versus deep water surf parameter for all data sets in the form of $y = \alpha e^{\beta x}$.

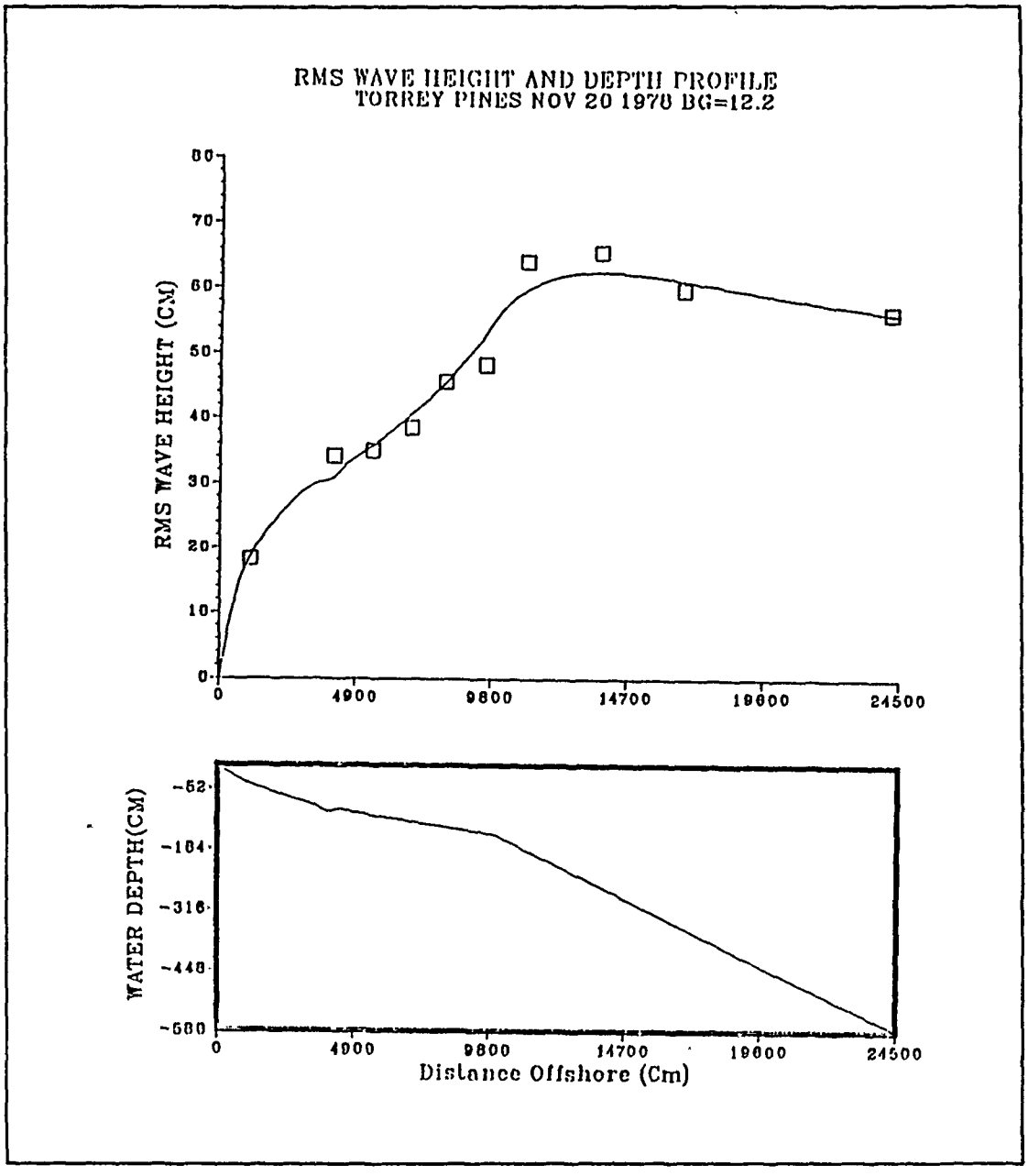


**Figure 8. Rms Wave Height and Depth Profile of Sample Torrey Pines Data:** Model predicted wave height versus November 20 1978 data. The solid line is the model predicted wave height while the individual points are the measured wave heights. The second plot shows the depth profile.

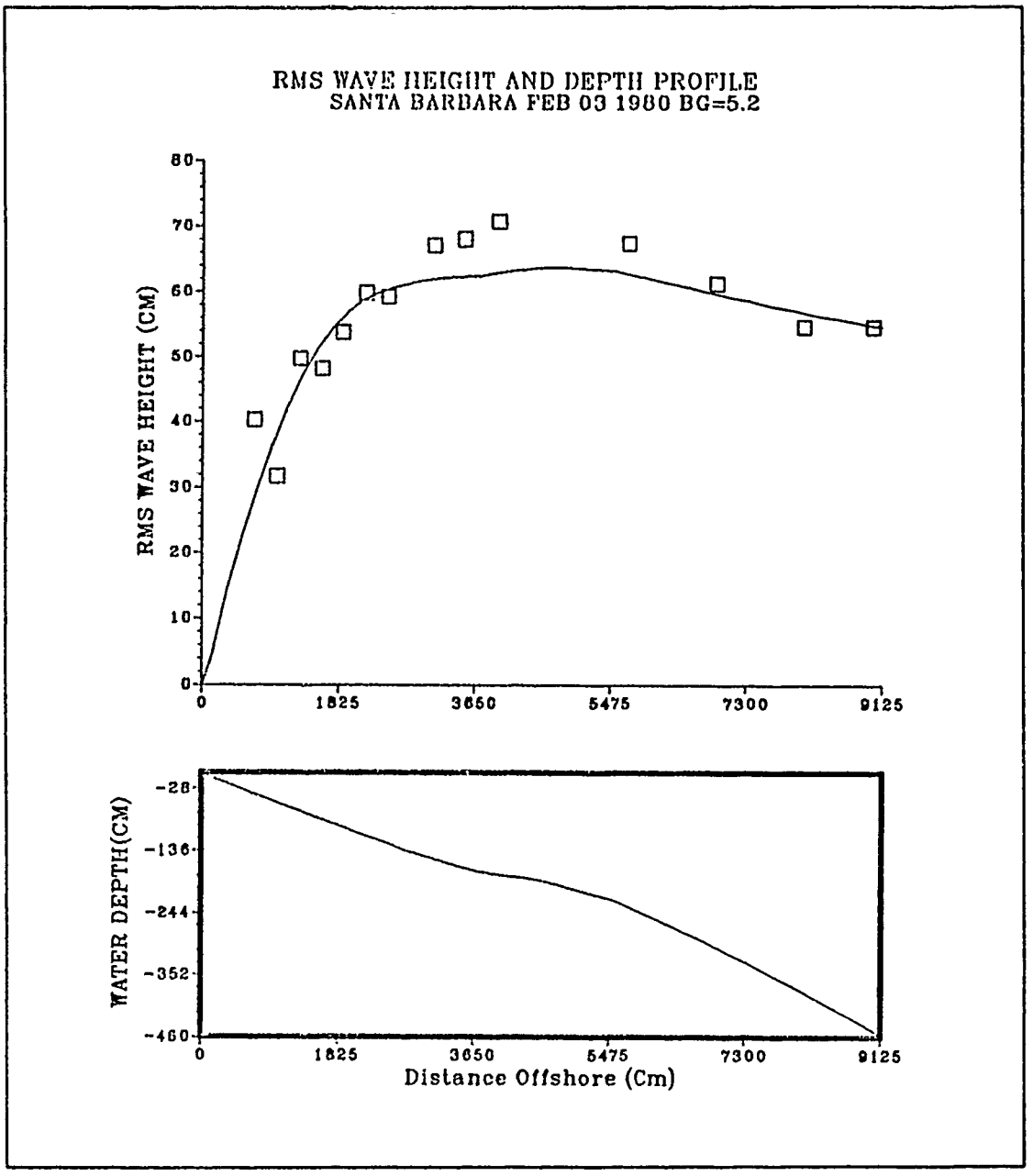


**Figure 9. Rms Wave Height and Depth Profile of Sample Santa Barbara Data:** Model predicted wave height versus February 03, 1980 data. The solid line is the model predicted wave height while the individual points are the measured wave heights. The second plot shows the actual depth profile.

Sallenger *et al.* (1985) investigated the dependence of wave height on local slope and depth. They found that $\gamma$ linearly increases with bottom slope in the form of:

$$\gamma = 3.2 \tan \beta + 0.30 \qquad [29]$$

They also concluded that the $\gamma$ coefficient was independent of the deep water wave steepness. The value of $\gamma$ was computed for all the data sets using the above relation. The coefficients obtained based on this relation ranged from 0.33 tc 0.48 with a mean of 0.40 . Their conclusion that $\gamma$ was independent of the deep water wave steepness was found also to be valid for the present data sets tabulated in chapter 3. The B values were computed by substituting the calculated $\gamma$ values into the combined BG parameter. The computed B parameter values in this manner ranged from 0.46 to 1.24 with a mean of 0.82 and a standard deviation of 0.17. This result shows that B is assigned reasonable values and agrees with the physics of the problem. These B parameter values showed an increasing trend with the deep water surf similarity parameter (see Figure 4) . As the breaker type shifts from spilling to plunging ($\xi_o > 0.4$), the B parameter values increase.

The longshore current model was run first neglecting turbulent mixing. Relatively high rms error percentages in the least square sense were obtained (See Figure 15 ). No matter how much $c_f$ was adjusted, it was not possible to obtain longshore current over the shore side of the bar where the waves reform and are no more breaking. Based on this result, it was decided to include turbulent mixing in the model. McDougal *et al.* (1986) investigated the influence of lateral mixing on longshore currents. They tested a variety of lateral mixing models and concluded that the longshore current profile is insensitive to the form of the mixing model. Therefore it was decided to use the lateral mixing model of Longuet-Higgins (1970b) which has the form of $\nu = \Lambda x \sqrt{gh}$ . Inclusion of the turbulent mixing increased the degree of the longshore current equation to the second. More reasonable results are obtained by including the turbulent mixing term (Figure 15).

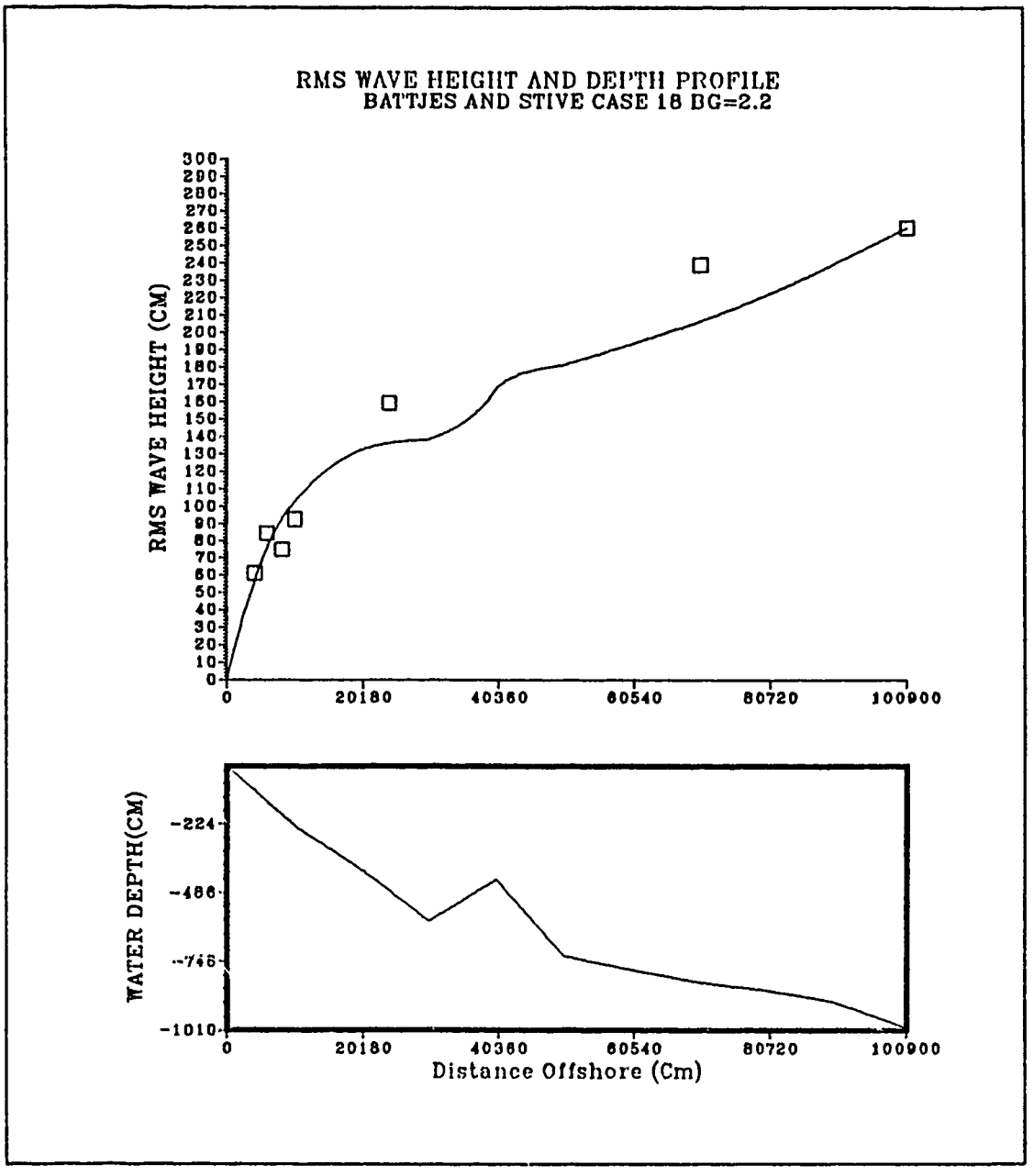


**Figure 10. Rms Wave Height and Depth Profile of Sample Battjes and Stive Data:** Model predicted wave height versus Case 18 data. The solid line is the model predicted wave height while the individual points are the measured wave heights. The second plot shows the actual depth profile.

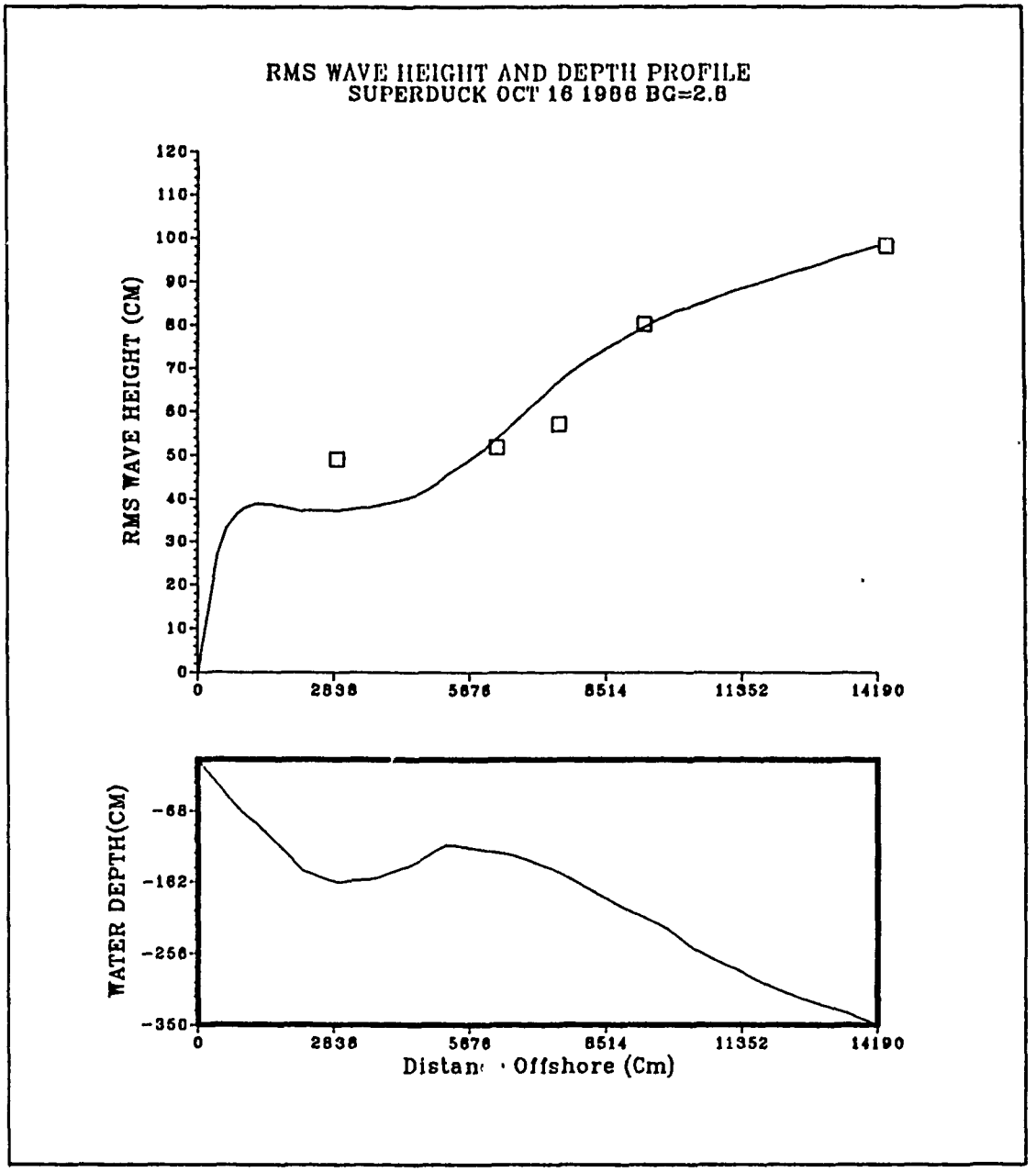


**Figure 11. Rms Wave Height and Depth Profile of Sample Superduck Data:** Model predicted wave height versus October 16, 1986 data. The solid line is the model predicted wave height while the individual points are the measured wave heights. The second plot shows the depth profile.

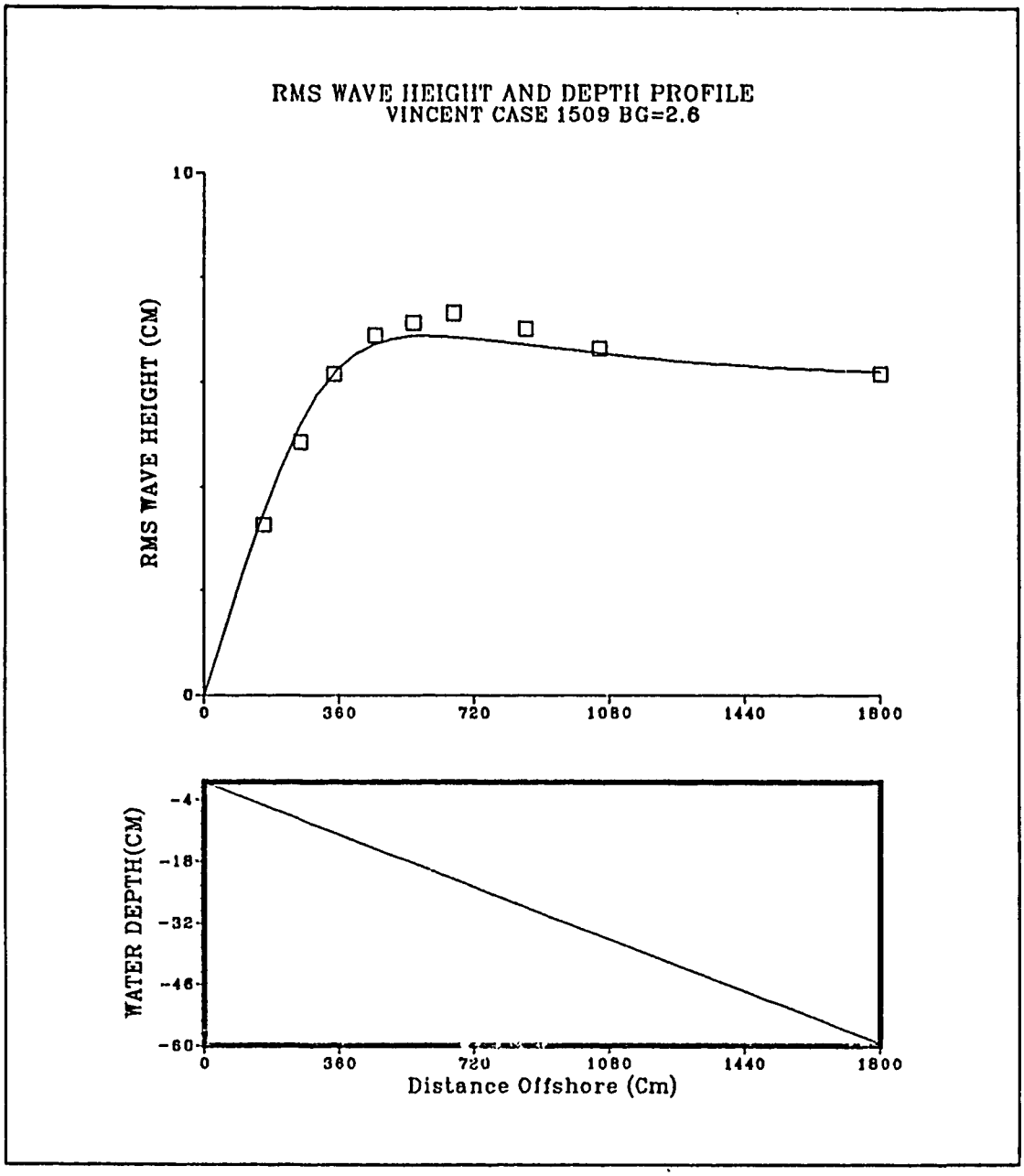


**Figure 12.** **Rms Wave Height and Depth Profile of Sample Vincent Data:** Model predicted wave height versus Case 1509 data. The solid line is the model predicted wave height while the individual points are the measured wave heights. The second plot shows the constant slope bottom profile.

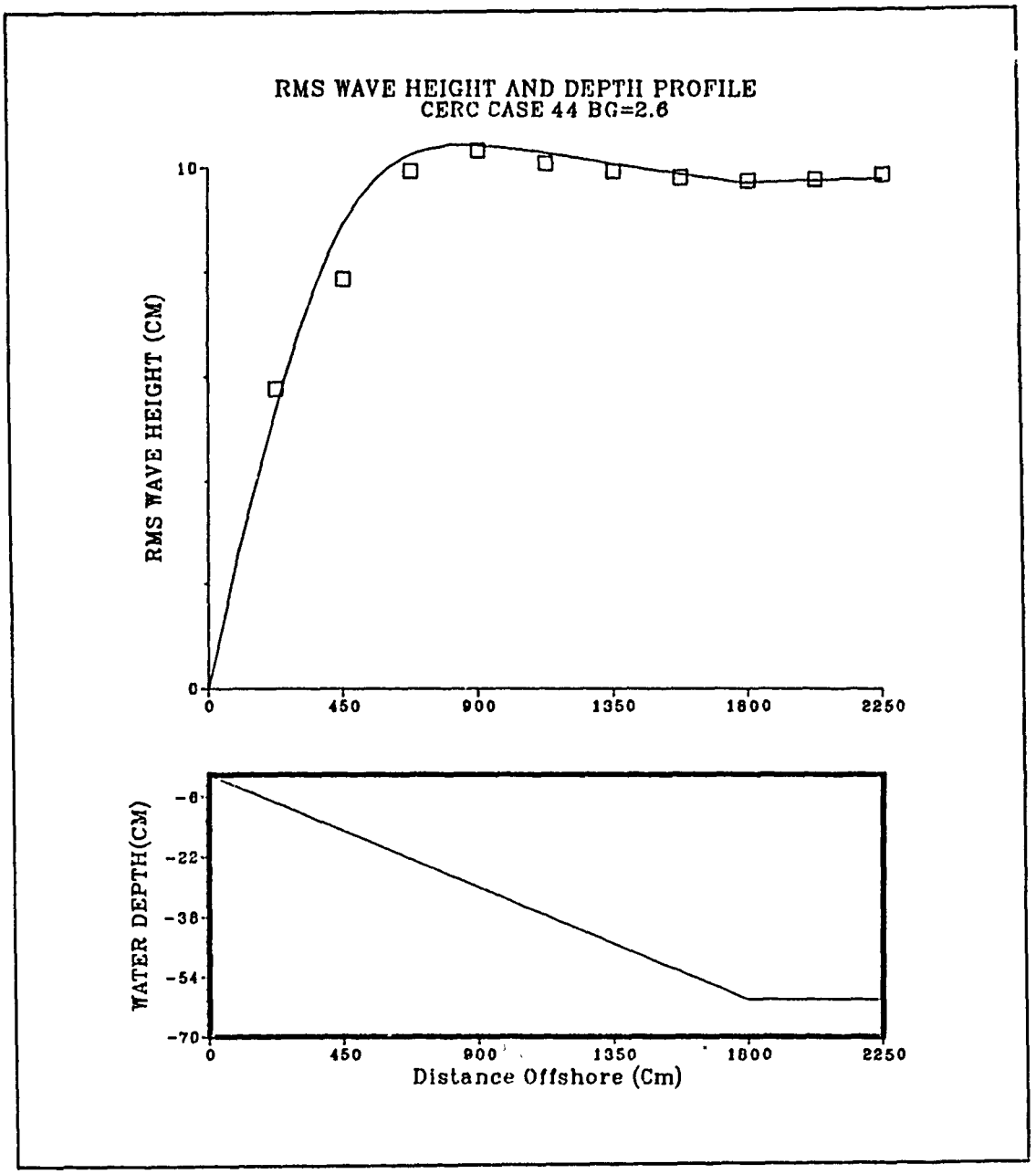


**Figure 13.** **Rms Wave Height and Depth Profile of Sample CERC Data Part (I):** Model predicted wave height versus Case 44 data. The solid line is the model predicted wave height while the individual points are the measured wave heights. The second plot shows the depth profile.

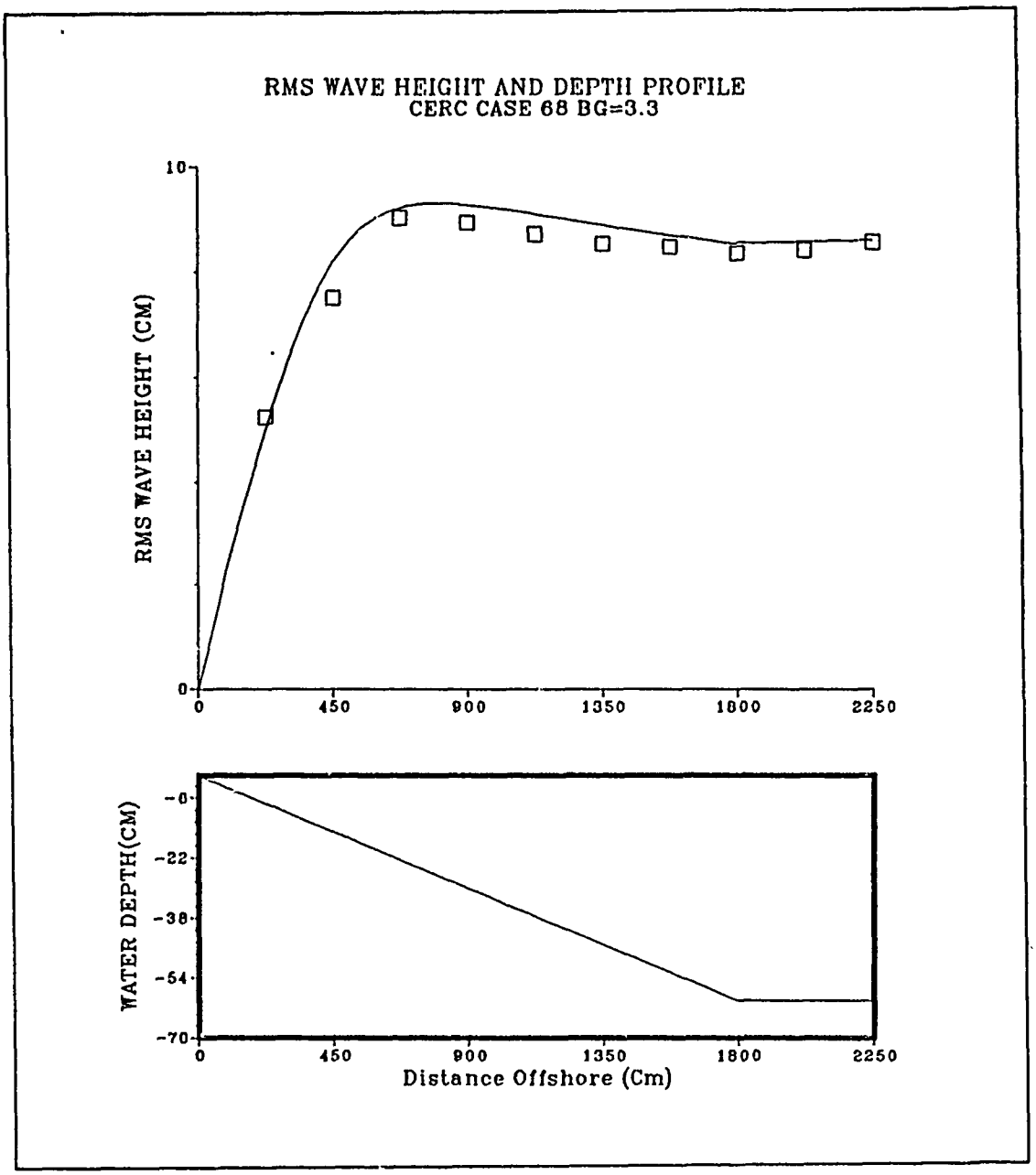


**Figure 14. Rms Wave Height and Depth Profile of Sample CERC Data Part (II):** Model predicted wave height versus Case 68 data. The solid line is the model predicted wave height while the individual points are the measured wave heights. The second plot shows the depth profile.

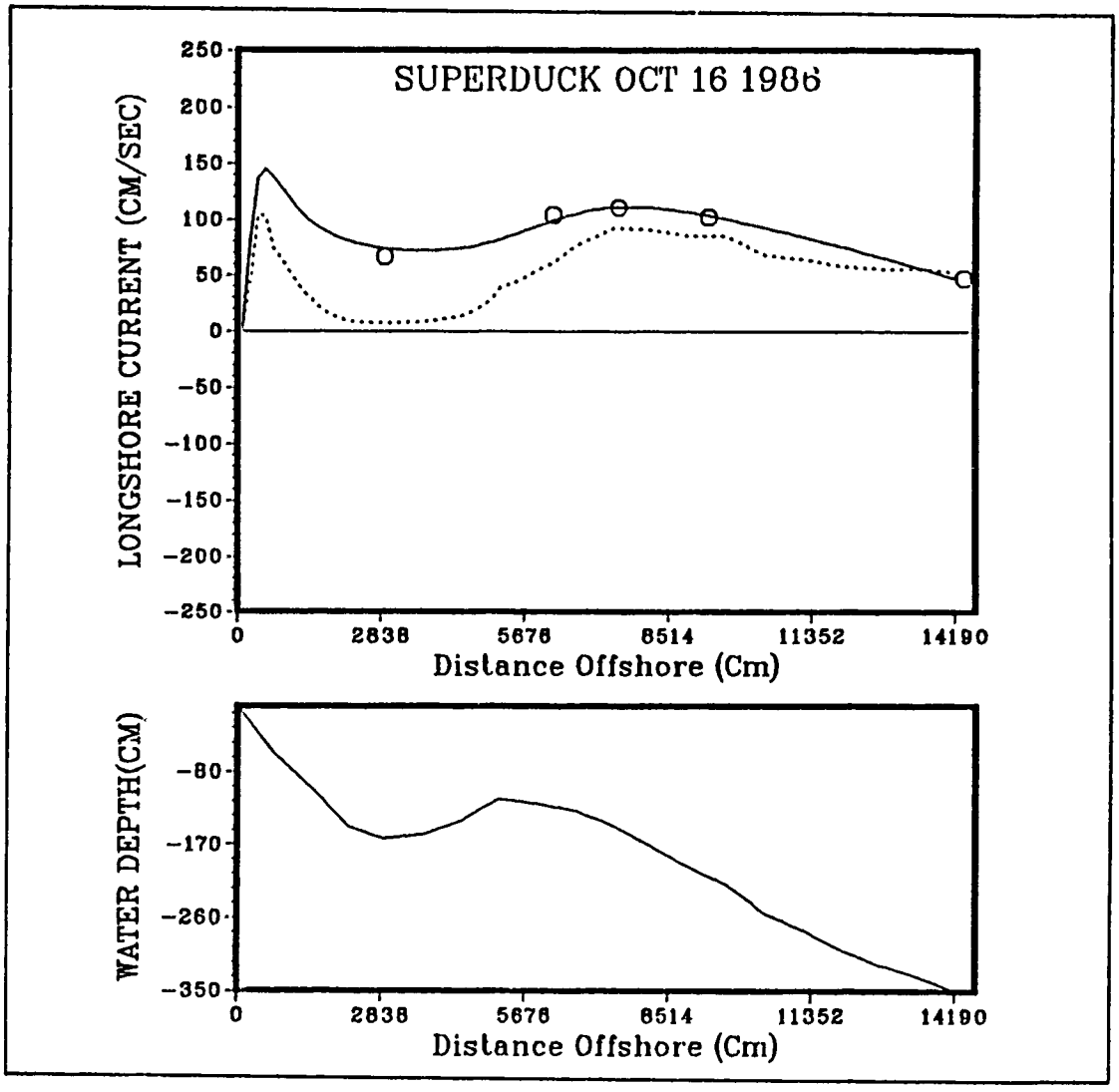


**Figure 15. Longshore Current and Depth Profile of Sample Superduck Data:** The dotted line indicates the model generated longshore current without turbulent mixing. The solid line is the model predicted current with turbulent mixing and the individual points are the measured wave heights. The second plot shows the depth profile. Notice that the velocities on shore side of the bar significantly change depending on inclusion or exemption of the turbulent mixing.

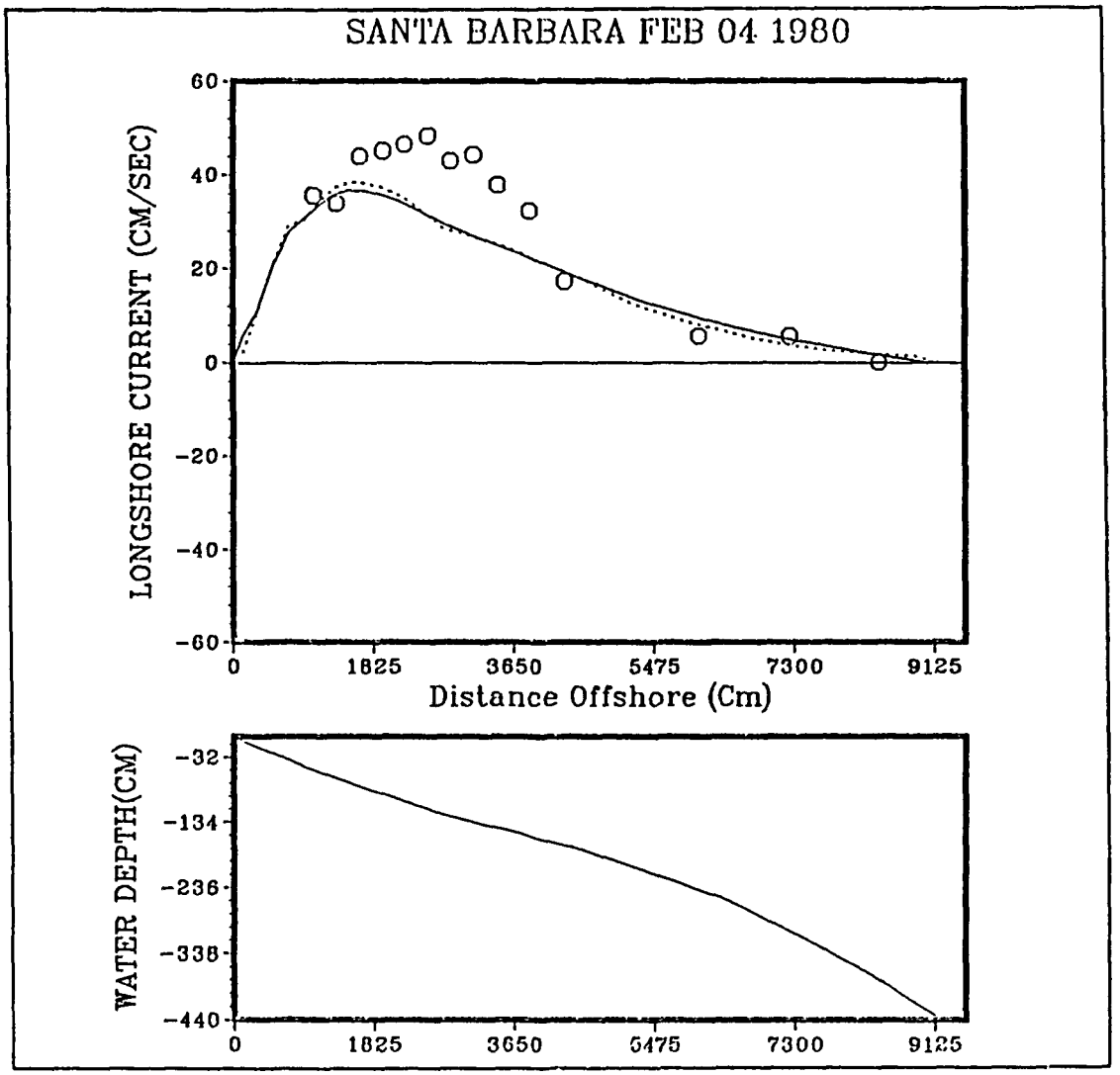


**Figure 16. Longshore Current and Depth Profile of Sample Santa Barbara Data:** The dotted line indicates the model generated longshore current without turbulent mixing. The solid line is the model predicted current with turbulent mixing and the individual points are the measured wave heights. The second plot shows the depth profile.

In the Santa Barbara data, the model generates a maximum longshore current closer to the shoreline compared with the maximum current measured (see Figure 16). This result was regardless of the inclusion or exemption of the turbulent mixing. Therefore, the inclusion of turbulent mixing to the model did not cause significiant improvement

for Santa Barbara longshore current data. The model comparision was found insensitive to the N value. Based on this result, turbulent mixing may be excluded in the model for planar beaches. As disscussed earlier this is not true for barred beaches. This would reduce the number of model parameters to be specified and also since the longshore current equation will stay in the first order, some cpu time will be saved. Planar beaches are more appropriate for Amphibious Warfare compared to barred beaches. Landings will not be made on barred beaches unless necessary. If a barred beach is to be chosen for landing, then the turbulent mixing should be included.

The mean value of the bed shear stress coefficient, $c_f$ for the present longshore current data is 0.006 and the mean lateral mixing coefficient is 0.0055. Since there is not enough longshore current data to obtain predictive relations for the model parameters, these mean values are suggested for use in model implementation. Longshore current magnitude is directly proportional to $c_f$. It should be recognized that, since the optimal $c_f$ values varied between 0.0025-0.009, the expected current magnitude can have significiant error using the suggested values. For generality, since it does not matter to include or exclude the turbulent mixing term for planar beaches, the model can run with these $c_f$ and N values regardless of the beach profile. These values should be checked as more longshore current data becomes available.

# V. SUMMARY AND CONCLUSIONS

In this study, the wave height transformation and longshore current models of Thornton and Guza (1983, 1986) are applied to a variety of wave conditions over planar and barred beaches for the purposes of testing and evaluation. 74 data sets of wave height transformation and 9 data sets of longshore currents are utilized. The model results are optimized in the least square sense to obtain the best fit to the data. The model coefficients in the wave transformation model, $\gamma$ a measure of saturated wave breaking and B a measure of breaking wave intensity, are combined into a single BG parameter. Based on data analysis, the combined BG parameter in the wave transformation model is found to be correlated with the deep water surf parameter. Therefore, this correlation can be used to predict the single model BG parameter in future model applications.

Testing the model using field and laboratory data shows that the wave transformation model is highly robust in describing the wave height distribution inside the surf zone. Varying the combined BG parameter one standard deviation from the mean of the 74 data sets, did not increase the rms error greater than 9%. Therefore it is concluded that model is not overly sensitive to the parameters.

The $\gamma$ parameter was calculated using the relationship by Sallenger and Holman (1985) and the B values were calculated from the BG parameter. The mean proportionality coefficient $\gamma$ for the whole 74 data sets was 0.4. The B parameter, which describes the intensity of wave breaking, appears also to be correlated with the deep water surf parameter. This is expected since the deep water surf parameter is used to predict breaker type, and B is a measure of breaking wave intensity.

For longshore current computations the turbulent mixing needs to be included over barred beaches, but for planar beaches its inclusion has an insignificant effect on the results. Therefore it is suggested the turbulent mixing be included in a general model for consistency. At present there is not a means for predicting the appropriate model parameters for longshore current computations. Therefore it is suggested the longshore current model be run with the mean values obtained for the bed shear stress and lateral mixing coefficients, 0.006 and 0.0055 respectively, regardless of the beach profile.

The model is operationally handy since it is only initialized by the offshore wave height, direction and period, which can be observed aboard the ship. The construction

of the model is quite simple, and does not require much computation time. Therefore the model can run on a personal computer with almost instant response.

## LIST OF REFERENCES


Battjes, J. A. , 1974: Surf Similarity. *Proceedings of the 14th International Conference Coastal Engineering , American Society of Civil Engineers, New york* 466-480

Battjes, J. A. and Stive M. J. F. , 1985: Calibration and Verification of a Dissipation Model for Random Breaking Waves. *J. Geophys. Res., 90, (c 5)* 9159-9167

Divorky, D. , LeMehauté, B. and Lin, A. , 1970: Breaking Waves On Gentle Slopes. *J. Geophys. Res., 75, (c 9)* 1681-1692

Gill M. J. , 1985: Test Evaluation of on Improved Sea, Swell and Surf Program. Master Thesis. *Naval Postgraduate School*

Horikawa, K. and Kuo, C. , 1967: A Study on Wave Transformation Inside the Surf Zone. *Proceedings of the 10th Coastal Engineering Conference, American Society of Civil Engineers,* 217-233

Hwang, L. S. and Divoky, D., 1970: Breaking Wave Setup and Decay on Gentle Slopes. *Proceedings of the 12th International Conference Coastal Engineering , American Society of Civil Engineers, New york* 377-389

LeMehauté, B. and R. C. Y. Koh, 1962: On Non-saturated Breakers Theory and the Wave Run-up. *Proceedings of the 8th International Conference Coastal Engineering , American Society of Civil Engineers, New york* 77-92

Longuet-Higgins, M.S., 1970a: Longshore Current Generated by Obliquely Incident Sea Waves. *J. Geophys. Res., 75* 6778-6789

Longuet-Higgins, M.S., 1970b: Longshore Current Generated by Obliquely Incident Sea Waves. *J. Geophys. Res., 75* 6790-6801

Longuet-Higgins, M.S. and Steward R.W., 1964: Radiation Stresses In Water Waves: A Physical Discussion, With Applications. *Deep Sea Research, II* 529-562

McDougal, W. G. , 1986: Influence of Lateral Mixing On Longshore currents. *Ocean Engineering, Vol. 13 No. 5* 419-433

Maron, M. J. , 1987: Numerical Analysis , A Practical Approach *Macmillan Publishing Co. , New York, Second Edition* 123-127

Meadows, G. A. , 1978: A Field Insvestigation of the Spatial and Temporal Structure of Longshore currents. *Purdue University, Department of Geosciences, Technical Report No. 6*

Nakamura, M., Shirashi, H. and Sasaki, Y., 1967: Wave Decaying Due to Breaking. *Proceedings of the 10th Coastal Engineering Conference, American Society of Civil Engineers,* 234-253

Sallenger, A., and R. Holman, 1985: Wave-Energy Saturation on a Natural Beach of Variable Slope. *J. Geophys. Res., 90* 11939-11944

Seelig, W.N., Ahrens, J.P. and Grosskopf, W.G., 1983: The Elevation of Duration of Wave Crests. *Coastal Engineering Research Center (CERC) Report No:83-1*

U.S. Army, 1984 : Shore Protection Manual. *U.S. Army Coastal Engineering Research Center (CERC) Vol. 1*

Smith, J. S. and Kraus C. N., 1988: An Analytical Model Of Wave-Induced Longshore Current Based On Power Law Wave Height Decay. *Coastal Engineering Research Center (CERC) Report No:88-3*

Stive, M. 1983 : Energy Dissipation in Waves Breaking on Gentle Slopes, *J. Coast. Eng.* 99-127

Thornton, E. B. and Guza, R. T., 1983: Transformation of wave height distribution. *J. Geophys. Res., 88, (c10)* 5925-5938

Thornton, E. B. and Guza, R. T., 1986: Surf Zone Longshore Currents and Random Waves: Field Data and Models. *J. Phys. Oceanography, 16, (7)* 1165-1178

Vincent , C. L., 1984: Energy Saturation Of Irregular Waves During Shoaling. *Unpublished Manuscript*

Whitford, D.J. 1988: Wind and Wave Forcing of Longshore Currents Across a Barred Beach. Dissertation, *Naval Postgraduate School*

Whitford, D.J. and Thornton E. B., 1989: Longshore Currents Over A Barred Beach. submitted to *J. Geophys. Res.*

Wu, C.-S., Thornton, E. B. and Guza, R. T., 1985: Waves and Longshore Currents: Comparision of a Numerical Model with Field Data. *J. Geophys. Res., 90, (C3)* 4951-4958

## INITIAL DISTRIBUTION LIST

| | | No. Copies |
|---|---|---|
| 1. | Defense Technical Information Center<br>Cameron Station<br>Alexandria, VA 22304-6145 | 2 |
| 2. | Library, Code 0142<br>Naval Postgraduate School<br>Monterey, CA 93943-5002 | 2 |
| 3. | Chairman (Code 68Co)<br>Department of Oceanography<br>Naval Postgraduate School<br>Monterey, CA 93943 | 1 |
| 4. | Chairman (Code 63Rd)<br>Department of Meteorology<br>Naval Postgraduate School<br>Monterey, CA 93943 | 1 |
| 5. | Dr. E.B. Thornton<br>Department of Oceanography<br>Naval Postgraduate School<br>Monterey, CA 93943 | 3 |
| 6. | Dr. C-S. Wu<br>Department of Oceanography<br>Naval Postgraduate School<br>Monterey, CA 93943 | 3 |
| 7. | Dz. Kd. Utgm. Nasuh Cacina<br>Nuri Pasa Mahallesi<br>64 sokak No:9 D:11<br>Zeytinburnu - Istanbul / TURKEY | 3 |
| 8. | Mr. S. Brand<br>NOARL, Bldg. 702<br>Naval Postgraduate School<br>Monterey, CA 93943 | 1 |
| 9. | Deniz Kuvvetleri Komutanligi<br>Personel Daire Baskanligi<br>Bakanliklar-Ankara / TURKEY | 1 |
| 10. | Seyir Hidrografi ve Osinografi Daire Baskanligi<br>Cubuklu - Istanbul / TURKEY | 3 |

11. Deniz Harp Okulu Komutanligi — 2
Tuzla - Istanbul / TURKEY

12. Ortadogu Teknik Universitesi — 1
Cevre Bilimleri
Ankara / TURKEY

13. Istanbul Teknik Universitesi — 1
Cevre Bilimleri
Istanbul / TURKEY

14. Dokuz Eylul Universitesi — 1
Cevre Bilimleri
Izmir / TURKEY

15. Director, Naval Oceanography Division — 1
Naval Observatory
34th and Massachusetts Avenue NW
Washington, DC 20390

16. Commanding Officer — 1
Fleet Numerical Oceanography Center
Monterey, CA 93943

17. Commanding Officer — 1
Naval Environmental Prediction Research Facility
Monterey, CA 93943

18. Ocean Science Directorate
Naval Ocean Research and Development Activity — 1
NSTL Station
Bay St. Louis, MS 39522

19. Office of Naval Research (Code 1121) — 1
800 N. Quincy Street
Arlington, VA 22217